NASA TECHNICAL TRANSLATION

NASA TT F-621

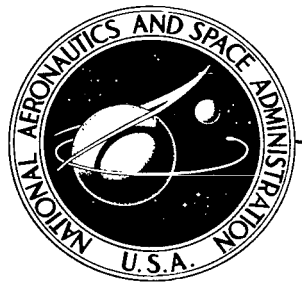

NASA TT F-621
C.1

LOAN COPY: I
AFWL (W
KIRTLAND AF
0068884
TECH LIBRARY KAFB, NM

ASTROMETRY AND ASTROPHYSICS, NO. 6, ANNULAR SOLAR ECLIPSE, MAY 20, 1966

A. A. Gorynya, Editor-in-Chief

"Naukova Dumka" Press, Kiev, 1968

NATIONAL AERONAUTICS AND SPACE ADMINISTRATION • WASHINGTON, D. C. • JUNE 1970

TECH LIBRARY KAFB, NM
0068884
NASA TT F-621

ASTROMETRY AND ASTROPHYSICS, NO. 6,

ANNULAR SOLAR ECLIPSE, MAY 20, 1966

A. A. Gorynya, Editor-in-Chief

Translation of "Astrometriya i Astrofizika, 6,
Kol'tseobraznoye Solnechnoye Zatmeniye, 20 Maya 1966 g"
Academy of Sciences of the Ukrainian SSR,
Main Astronomical Observatory,
"Naukova Dumka" Press, Kiev, 1968

NATIONAL AERONAUTICS AND SPACE ADMINISTRATION

For sale by the Clearinghouse for Federal Scientific and Technical Information
Springfield, Virginia 22151 – CFSTI price $3.00

ANNOTATION

This collection contains data from observations of the annular /4 solar eclipse on May 20, 1966 gathered by an expedition of the Main Astronomical Observatory of the Academy of Sciences of the Ukrainian SSR.

This volume also describes the equipment and instruments used for the observations and discusses the results of interpretation of the photographs obtained to determine the profile shape of the Moon and coordinate corrections.

This issue is intended for our scientific colleagues at the observatories and graduate and undergraduate students specializing in astronomy.

BOARD OF EDITORS:

Ye.P. Fedorov *(Chairman)*,
Z.N. Aksent'yeva, N.P. Barabashov, A.F. Bogorodskiy *(Vice-Chairmen)*
A.A. Gorynya *(Chief Secretary)*
I.K. Koval', I.G. Kolchinskiy, V.P. Tsesevich, A.A. Yakovkin.

A. A. Gorynya -- Editor-in-chief.

TABLE OF CONTENTS

INTRODUCTION..... 1

I.M. Demenko, A.S. Duma and D.P. Duma:

THE LUNAR PROFILE ACCORDING TO OBSERVATIONS OF THE ANNULAR ECLIPSE OF MAY 20, 1966..... 3

Observations and Equipment..... 3
Measurements, Orientation of the Plates and Analysis of the Errors..... 8
Reduction of the Measurements and Comparison of the Profiles.....10
Analysis of the Profiles and Conclusions.....18
References.....26
Application.....27

I.M. Demenko, A.S. Duma, D.P. Duma and V.S. Kislyuk:

DETERMINING CORRECTIONS FOR THE COORDINATES OF THE MOON ACCORDING TO OBSERVATIONS OF THE ANNULAR SOLAR ECLIPSE ON MAY 20, 1966.....43

References.....50

N.A. Vasilenko:

THE ACCURACY OF THE DETERMINATION OF THE COORDINATES OF THE SITE AND THE MOMENTS OF OBSERVATION OF THE ANNULAR SOLAR ECLIPSE OF MAY 20, 1966.....51

References.....53

K.Ye. Skorik:

DESCRIPTION OF THE HIGH-SPEED CASSETTE AND SHUTTER USED TO OBSERVE THE ANNULAR SOLAR ECLIPSE OF MAY 20, 1966.....54

The Cassette Section.....55
The Shutter.....56

INTRODUCTION

Annular solar eclipses are comparatively rare phenomena in /7* nature. During the annular phase the Moon is projected onto the surface of the Sun, and the observer sees the full lunar disk, which is impossible to observe from the Earth under any other circumstances. Therefore, annular solar eclipses offer an opportunity to observe the full lunar profile; it is essential to know its outline to determine lunar coordinates from observation. These observations may be used for solving a number of astronomical problems, including, for instance, a study of the Earth's rotation from the movement of the Moon, determination of the orientation units of the systems from the fundamental catalogs, determination of the coordinates of points on the Earth's surface which are separated by considerable distances in order to study the shape of the Earth, determination of the epheremis time, study of the movement, rotation and the three-dimensional geometric shape of the Moon, as well as a number of practical problems associated with the conquest of outer space, etc.

The successful solution to these problems involves certain difficulties. As we know, in practice we determine the coordinates of the center of the most probable circle which may approximately represent the outline of the Moon. However, the point found in this manner does not agree with the center of mass, which partially explains the systematic divergence between theory and observation. This contradiction can be easily overcome if we know the geometry of the full profile for different optical librations. The use of lunar observations, when only half of the profile is visible, will not lead to the desired results, since the center of the figure does not retain its position on the Moon under various optical librations. Thus, photographing the annular solar eclipse is an important and necessary step in determining the position of the center of the lunar mass from observation. Therefore the Main Astronomical Observatory of the Academy of Sciences of the Ukrainian SSR organized an expedition to observe the annular solar eclipse on May 20, 1966.

The annular phase of the solar eclipse on May 20, 1966 began near the equator in the Atlantic Ocean. Then the path passed through northwest Africa, the Aegean Sea, the northwest part of Turkey, the /8 Black Sea, the Northern Caucasus, the Caspian Sea, Lake Balkash and Mongolia, ending in China. The eclipse was visible in Africa and

*Numbers in the margin indicate pagination in the foreign text.

Turkey for less than one second; when it entered the Soviet Union it was visible for about one second, and as it approached the Chinese border it could be seen for about 30 seconds.

The observatory expedition selected a site for observation in the "Kyzyl-Tan" Sovkhoz of the Aksu District of the Alma-Ata Region. The annular phase could be seen here for about 26 seconds and the width of the path, by preliminary computation, was about 22 km. The expedition was required to obtain photographs of the solar eclipse by using two coronagraphs for studying the shape of the visible profile and for determining corrections to the lunar coordinates. There were eight persons in the expedition: Director of the Department of Solar Physics, E.A. Gurtovenko; Chief Mechanic of the Observatory, K.Ye. Skorik; Junior Science Assistant, D.P. Duma (beginning of the expedition); Senior Engineers N.A. Vasilenko and A.S. Rakhubovskiy; Student V.S. Kislyuk; Engineers A.S. Duma and L.N. Miz'. The expedition completed its projected program.

In the present collection we have published the basic results obtained from processing the data from the annular solar eclipse on May 20, 1966 as well as certain data on the equipment and the observational conditions.

THE LUNAR PROFILE ACCORDING TO OBSERVATIONS OF THE ANNULAR ECLIPSE OF MAY 20, 1966

I.M. Demenko, A.S. Duma and D.P. Duma

Observations and Equipment

To observe the annular solar eclipse of May 20, 1966, an /9
expedition of the Main Astrophysical Observatory of the Academy of Sciences of the Ukrainian SSR traveled to the "Kyzyl-Tan" Sovkhoz in the Aksu District of the Alma-Ata Region. The observation area was located on the left bank of the Aksu River 300 m northeast of the central farmstead of the sovkhoz. The terrain was unobstructed in all directions except for two old buildings near the instruments, which were arranged in such a way that not only did they not obstruct our observations, but they could even be used to shield the chronometer and certain other pieces of equipment from dust and the sun.

The expedition was held in the spring. During the entire period we encountered temperatures which were low for this area. At night the temperature dropped from +5 to 0°C; in the daytime, it varied between +5 and +30°C. Of the time spent on the expedition, on three days the weather was absolutely clear and on the remaining days clouds appeared which lasted all day. However, there was sufficient sun to set up the equipment and check it. On May 20, the day of the eclipse, it was slightly cloudy in the morning. After noon the sky cleared and, before the eclipse, was cloudless, except for some slightly noticeable cirrus clouds on the horizon. After the third contact, scattered clouds appeared, the density of the cirrus clouds increased, and theybecame significant in the zone of the eclipse. In general, during the eclipse the weather was suitable for operating the coronagraph and the photographic material.

Our operations were greatly hindered by strong, dusty southwest winds which blew throughout most of the expedition. These winds were the basic obstacle to operation of the optical equipment and the instruments. To keep excessive dirt off the mirrors and lenses, we made lens covers which covered the optical equipment and were removed only to focus the image on the plates. The fact that the surface layer of the atmosphere was so dusty forced us to keep the instruments closed and covered; this was extremely inconvenient, particularly in positioning and aligning the coronagraphs. The measures taken could not guarantee that the equipment

would not get dirty, so we repeatedly washed and cleaned the optical equipment and the instruments. On May 19, the glass, lenses and /10
mirrors had undergone their final cleaning, and before the eclipse we uncovered them for a short period of time. The wind did not abate on the day of the eclipse. To prevent the coelostat from shaking in the wind, we built a canvas enclosure. After noon and just before the eclipse the wind died down slightly.

The task of the expedition was to photograph the partial annular phases of the eclipse, to calculate corrections to the coordinates and to determine the shape of the lunar profile. The expedition was equipped with two coronagraphs with focal lengths of F = 20 m and 10 m and lens diameters of 20 cm and 10 cm, respectively. To determine the coordinates of the observation point and record the time, we included a two-second universal instrument, stellar and mean chronometers, a radio transmitter, a pulse attachment, and printing and marking chronographs [1]

For the 12-meter coronagraph we used a special cassette with 20-30 photographic plates, 18 × 24 cm [2]. The construction of the cassette section allowed us to photograph the eclipse with 2-3 second intervals between exposures. The lens of the 12-meter coronagraph was photovisual; therefore, we installed a yellow filter 20 cm in front of the photographic plate.

For the 10-meter coronagraph we used cassettes from an NAFA-50 camera. The lens and the shutter of the NAFA-50 were detached from the cassette section, and the electrical circuit and the mechanical subassemblies were arranged in such a way that when a double-contact button was pushed, a wide piece of film would be drawn out then pressed by the stage onto a plane-parallel glass plate, whose rear face was located in the focal plane of the lens. This allowed us to take pictures with intervals of 2-4 sec between exposures. The cassette section of the NAFA-50 was firmly attached to a metallic plate and fixed on a brick foundation.

Disc shutters with radial slits [2] were attached to both coronagraphs in front of the cassettes about 40 cm from the focal plane. Since the disc was rotating, the image was exposed non-simultaneously. Therefore, the rotation rate of the discs was chosen so that the shift in the image due to the inherent motion of the Moon would not exceed 0.01" - 0.02".

The 12-meter coronagraph was equipped with a standard AZS-2 /11
device. The mirror was rotated using the electric motor of the printing chronograph. The 10-meter coronagraph was equipped with a specially-prepared coelostat device, with a mirror set in motion by a CD-54 electric motor. The proper rotation rate was achieved by the choice of the diameters of two drive pulleys. The tubes of the coronagraph were made of veneer coated inside with carbon black. Diaphragms were installed every 1.5 m. The outside of the tubes was wrapped in thick black paper and then painted white. For

ease of operation, the cassettes and shutters with the photographic materials were placed in lightproof tents.

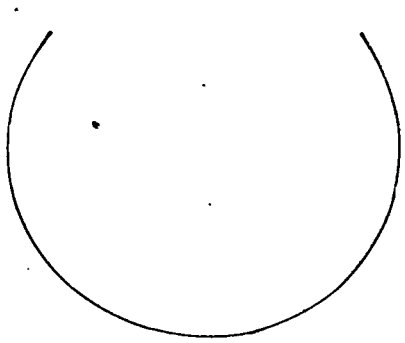

Fig. 1. Annular Phase (12-Meter Coronagraph).

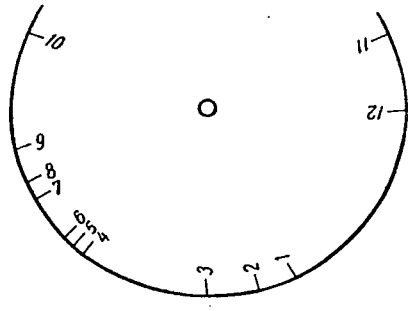

Fig. 2. Annular Phase (10-Meter Coronagraph).

The Pictures Show the Details Used for Orientation of the Detail.

For the several days preceding the solar eclipse we took detailed photographs of the Sun. Analysis of the photographs showed that the most suitable films were "Gelb Rapid" and "Izoortokhrom". With the discs rotating at about 3 rps, the less-sensitive diapositive films produced weak images. It is not advisable to decrease the shutter speed significantly, since the elongation of the image of the Moon due to its inherent motion would become considerable. The rapid rate at which the photographs were taken allowed us to obtain a large number of photographs during the annular phase, which lasted only 26 sec.

The photographs on the 10-meter coronagraph were taken on isopanchromatic film with a photosensitivity of 130, according to the All-Union State Standard 0.85, and a contrast coefficient of 3.0; /12 the optical density of the film was 0.06 and the resolution was 250 lines/mm. The difference in the longitudinal and lateral shrinkages of the film after photochemical processing was 0.01%.

The observation program called for uniform photographs of the eclipse to be taken from the first to the fourth contact. On the 12-meter coronagraph, the interval between exposures was 5 min; the interval on the 10-meter coronagraph was 2 min. Between the second /13 and third contacts, photographs were taken at the maximum rate. The photographs of the solar eclipse of May 20, 1966 were developed in Kiev. The material obtained was found to be quite suitable for interpretation. The 12-meter coronagraph took a total of 10 and the 10-meter coronagraph took a total of 9 photographs of the annular phase and about 80 photographs suitable for measuring the crescents (Figs. 1 - 6). After the film was developed, we could see that the rings were not complete. The rings obtained on the

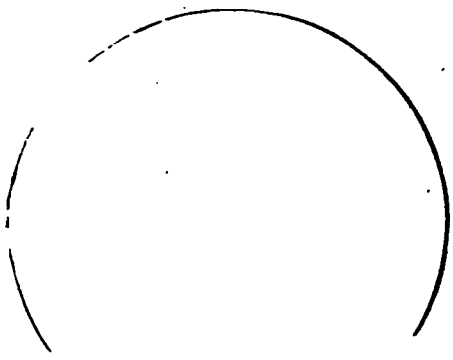

Fig. 3. Annular Phase with "Bailey Beads" (10-Meter Coronagraph).

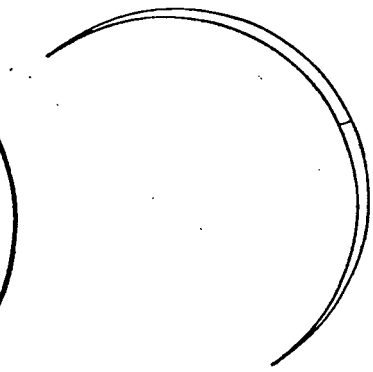

Fig. 4. Partial Crescent Phase (12-Meter Coronagraph).

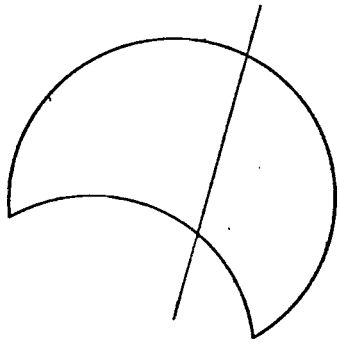

Fig. 5. Partial Crescent Phase (10-Meter Coronagraph).

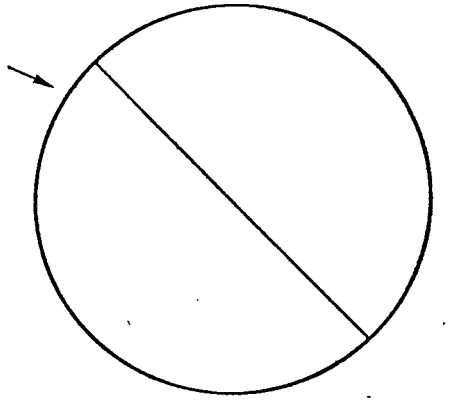

Fig. 6. Initial Moment of the Eclipse. The Arrow Indicates the Wane (10-Meter Coronagraph).

TABLE 1.

No.	Number of Plates or Films	Measurements Made by:	Length of the Measuring Arc	P	Number of Orientation Points	σ_p
			Plates			
1	32	V.S. Kislyuk	319.8°-0°-213.8°	113.8°-T	9	±0.51°
2	34	V.S. Kislyuk	311.8°-0°-213.8°	-72.2°+T	13	0.35°
3	35	D.P. Duma	311.0°-0°-213.0°	167.0°-T	8	0.26 °
4		A.S. Duma	311.0°-0°-213.0°	167.0°-T	8	0.26°
5		I.M. Demenko	311.0°-0°-213.0°	167.0°-T	8	0.26°
6	36	I.M. Demenko	316.0°-0°-219.0°	283.0°-T	15	0.31°
7	38	A.S. Duma	310.0°-0°-214.6°	24.6°-T	13	0.25°
8	39	V.S. Kislyuk	313.4°-0°-213.4°	243.4°-T	12	0.40°
9	40	V.S. Kislyuk	311.5°-0°-213.5°	99.5°-T	14	0.21°
10	52	A.S. Duma	187.2°-346.2°	277.2°-T	9	0.40°
11	54	D.P. Duma	189.4°-344.4°	284.4°-T	9	0.31°
12		A.S. Duma	189.4°-344.4°	284.4°-T	9	0.31°
13		I.M. Demenko	189.4°-344.4°	284.4°-T	9	0.31°
			Films			
14	66	A.S. Duma	358.2°-0°-238.2°	96.2°-T	12	±0.21°
15	67	I.M. Demenko	357.9°-0°-237.9°	359.9°-T	8	0.13°
16	68	A.S. Duma	357.7°-0°-243.7°	183.7°-T	13	0.27°
17	69	I.M. Demenko	356.4°-0°-245.4°	277.4°-T	13	0.26°
18	70	D.P. Duma	353.7°-0°-247.7°	0.7°-T	8	0.14°
19	71	A.S. Duma	356.1°-0°-248.1°	93.1°-T	9	0.24°
20	72	I.M. Demenko	355.3°-0°-247.3°	296.3°-T	10	0.25°

Note: σ_p is the mean square error in determining one detail.

12-meter coronagraph encompassed only 265° and those on the 10-meter coronagraph about 255°. The missing parts of the ring were obscured by the mountings of the filters. However, the photographs of the eclipse obtained between the second and third contacts were quite suitable for solving the problem of the shape of the lunar profile, and the crescents photographed during the minutes after the third contact supplied the missing portions of the profile.

Measurements, Orientation of the Plates and Analysis of the Errors

We determined the geometric shape of the lunar profile and corrected the lunar coordinates based on 14 photographs of the annular phase (seven plates and seven films) and two plates with images of crescents obtained during the few minutes after the third contact. For five rings (three plates and two films) and two crescents, we measured the radius-vectors and the artificial marker lunar limb-solar limb every 1°; for the rest of the plates and films we measured every 2° according to the position angle. All measurements were made on a UIM-22 all-purpose measuring microscope. Before the measurements were taken, we checked the scalar delineations and the shape of the guidelines of the UIM-22. Using the standardization method [3], we compared the scalar delineations with a standard scale. We studied the linearity of the scales using a control device, an extended frame with a metallic fiber. The results of measurements made independently by A.S. Duma and I.M. Demenko were compared and compiled. An investigation showed that corrections to the scalar delineations for the curvature of the guidelines did not exceed two microns. The small values of the corrections obtained as compared with the errors made in determining them, their random nature and the permissible measurement accuracy of the UIM-22 allows us to ignore them from now on.

Four different people measured the photographs. This was done /15 in each position angle on the artificial marker by two measurements and on the edges of the Moon and the Sun by four measurements. To check the agreement of the results obtained by different people, the ring in the 35th plate was measured independently by three people. In the worst case, the discrepancy in the mean calculations did not exceed 10 μ; i.e., less than 0.2″. To measure the photograph, the position circle was rotated in one direction, the direction being varied for different photographs. The accuracy of the measurements was estimated using two arbitrarily chosen photographs. For the 34th plate and the 70th film, the mean square errors of one measurement of the edge of the Moon were 0.004 and 0.005 mm, respectively; i.e., less than 0.1″ in both cases. The results of the measurements of all plates and films are given in the appendix.

We had intended to orient the plates according to the trails of the Sun or stars which, according to the program, we were to have obtained after the eclipse. However, after the eclipse the weather became worse. On the first evening we were not able to

obtain satisfactory photographic results. The following day was also overcast so we dismounted the instruments. We decided to orient the plates using the "Paris Observatory Atlas of Lunar Profiles" [4]. To do this, before our measurements we chose 10-20 characteristic details of lunar relief in each photograph and measured their position angles. These details were identified using their images on several profiles of the limb zone with librations close in value to the librations of the eclipse of May 20, 1966. If the detail could be identified with certainty, then from the Weimer profile we took the value of the position angle P of the chosen detail with an accuracy of 0.1°. By comparing the angle T in the coordinate system used in the measurements with the value P of these details on the Weimer profiles, we found the relationships for the conversion from the measured to the required position angles. Before we began the calculation, we selected the north pole of the Moon with zero libration. The angles were calculated from the north pole through the east. Table 1 contains the information on the orientation of the plates and the relationships for converting from measured to position angles in the coordinate system used.

The determination of the shape of the lunar profile is a subtle problem. Therefore, we must use high-quality materials and our measurements must have a high level of accuracy. The ultimate data used to determine the geology of the profile must not contain sig- /16
nificant systematic errors. A realistic upper limit to these errors in this case would be 0.2". Therefore, before our interpretation we attempted to evaluate the observational material obtained; i.e., we evaluated certain possible systematic errors. These include emulsion shifts, tilted plates, turbulence aberration, diffraction, irradiation, warped films and other effects.

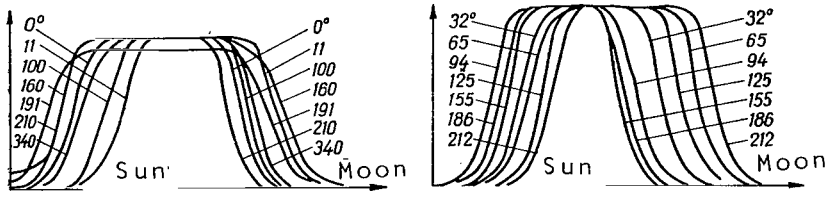

Fig. 7. Blackening Increase Curves for the Limbs of the Sun and the Moon.

Emulsion shift may be uniform over the entire field and random in a particular section. In the first case, the geometry of the object is easy to determine; in the second case, it is more difficult. In the photographs of the solar eclipse of May 20, 1966, the ring was not very wide; therefore, with permissible accuracy we may assume that the limbs of the Sun and the Moon vary identically due to emulsion shifts which can be easily detected by comparison with the measured radius vectors of the Sun in various position angles. We conducted this kind of operation during the investigation and discovered that this source of error was absent.

Tilting of the plate relative to the optical axis is dangerous, since the thickness of the ring may be increased in individual sections. A simple calculation showed that a noticeable effect occurs if the angle of inclination is not less than 10°. In our case, the plates and films were set with an accuracy one order of magnitude higher.

For short exposures, atmospheric turbulence causes nonuniform shifts in certain sections of the limb. If the exposure is longer, the action of turbulence is less dangerous and can be detected as blurring of the limb. The effect of turbulence can be detected by successive comparisons between the photographs. We conducted /17 such an investigation and will present the results later. In addition, for two rings (the 36th plate and the 69th film), on a microphotometer we obtained curves for the blackening increase for the solar and lunar limbs through 20-25° (Figs. 7a, b). It can be seen from the figures that the slopes of the blackening front are identical in all position angles, which once again indicates the absence of limb blurring due to atmospheric turbulence and the absence of systematic errors caused by tilting the plate relative to the optical axis, etc.

Irradiation in the emulsion of the photographic plates and films may significantly alter both individual details and whole sections of the ring. It is very difficult to take irradiation into account. A thorough examination of the action of irradiation was made in [5]. The authors derived criteria for an approximate estimate of the systematic errors caused by this effect. It follows from [5] that irradiation exerts a strong influence on the configuration of the relief in the case of overexposures. The photographs of the eclipse of May 20, 1966 were obtained with normal exposures; therefore, they have normal densities, and certain ones even have densities which are too low. As we know, in this case, the danger of significant distortion of the profiles is much less than in the case of an overexposure. However, we must bear in mind that the 1966 ring was narrow. Its width at the moment of maximum convergence of the centers of the Sun and the Moon was only one order of magnitude greater than the effect of irradiation. The influence of irradiation may be significant in individual sections of the ring at those moments when the ring is nonsymmetrical. Therefore, to determine the shape of the profile we chose only central photographs; i.e., those in which the ring was almost symmetrical.

We will not discuss here the nature of the action of other sources of error.

Reduction of the Measurements and Comparison of the Profiles

In Figure 8, let S be the center of the solar disc and L the center of the lunar disc. The distance between them $SL \ll SA$. We

will assume that the thickness of the ring is the difference between the radius vectors of the Sun and the Moon:

$$AB=SB—SA. \tag{1}$$

In practice, we use an artificial point S' which does not coincide with S. Therefore, the width of the ring according to the measurements is

$$A'B=S'B—S'A'. \tag{2}$$

From triangles SBS' and $SA'S'$ we can determine $S'B$ and $S'A'$: /18

$$\begin{aligned} S'B^2 &= SB^2 + SS'^2 - 2\,SB\cdot SS'\cos BSS', \\ S'A'^2 &= SA'^2 + SS'^2 - 2\,SA'\cdot SS'\cos A'SS' \end{aligned} \tag{3}$$

or with an accuracy of up to the small first-order terms

$$\begin{aligned} S'B &= SB\left(1+\frac{SS'^2}{2\,SB^2}-\frac{SS'}{SB}\cos BSS'\right), \\ S'A' &= SA\left(1+\frac{SS'^2}{2\,SA^2}-\frac{SS'}{SA}\cos A'SS'\right). \end{aligned} \tag{4}$$

Then the width of the ring Δh_i based on (4) may be computed according to the formula

$$\begin{aligned} \Delta h_i = S'B - S'A' = SB - SA - SS'(\cos BSS' - \\ - \cos A'SS') + \frac{1}{2}\left(\frac{SS'^2}{SB}-\frac{SS'^2}{SA}\right). \end{aligned} \tag{5}$$

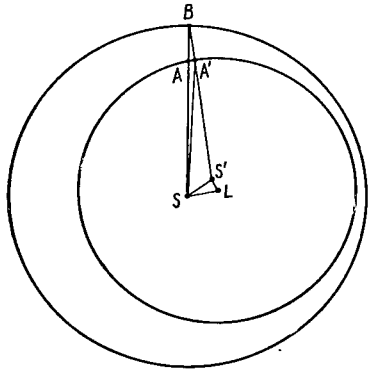

Fig. 8. Diagram for Determination of the Width of the Ring.

If the discrepancy between the artificial point and the true center of the Sun $SS' \leq 1$ mm, which is true in our measurements, and $SB \approx SA = 50$ mm, it is easy to see that the difference $AB - A'B < 0.001$ mm $\approx 0.02''$. We did not introduce these small reductions into the measured width of the ring $A'A$. The discrepancy between the artificial point and the true center of the Sun was also derived from the corrections to the measured position angles. For photographs of the 1966 eclipse the corrections do not exceed 0.2° if we observe the abovementioned accuracy in plotting the artificial point.

The proposed method of orienting the photographs does not allow us to take these corrections into account, since they are partially included in our determination of the zero point for computing the position angles on the basis of details which are uniformly distributed over the limb

The next step is to include the mean thickness Δh for a given photograph from the ring width at all position angles. This thickness can be found using the formula

$$\Delta h = \frac{1}{n}\sum_{i=1}^{n}\Delta h_i, \tag{6}$$

where n is the number of measurements. The altitude of a point on /19 the limb ΔH_i in a given position angle is computed according to the formula

$$\Delta H_i = \Delta h - \Delta h_i. \tag{7}$$

The altitudes of the lunar terrain which we found in this way are relative to the probable circumference of the Sun and contain corrections for the discrepancy between the centers of the Sun and the Moon, the nature of which is easy to express analytically and accurately to the small second-order terms

$$\Delta H_i = \Delta H_i' + \sigma\cos(P_i - \alpha) + \frac{\sigma^2}{2r}\sin^2(P_i - \alpha), \tag{8}$$

where σ is the distance between the centers of the Sun and the Moon; α is the angle which determines the direction of σ.

To reduce ΔH_i to the probable circumference whose center coincides with the center of the Moon, for each photograph we solved a system of conditional equations such as

$$\Delta x\cos P + \Delta y\sin P + \Delta H_0 = \Delta H_i. \tag{9}$$

After this operation, the altitude from the solar limb in a coordinate system with its origin at the center of the Moon is

$$\Delta H_i' = \Delta H_i - \sigma\cos(P_i - \alpha) - \Delta H_0, \tag{10}$$

where

$$\sigma = \sqrt{\Delta x^2 + \Delta y^2},$$

$$\alpha = \arctan\frac{\Delta y}{\Delta x}.$$

The graphs in Figures 9 and 10 show the heights of the relief of the limb zone obtained in this manner. Along the abscissa we have plotted the position angle P, and along the ordinate the value

of ΔH_i. A comparison of individual profiles based on the plates and films showed satisfactory agreement, but we detected a noticeable discrepancy between the profiles of two coronagraphs. The systematic discrepancy in individual sections reached a value of 1".

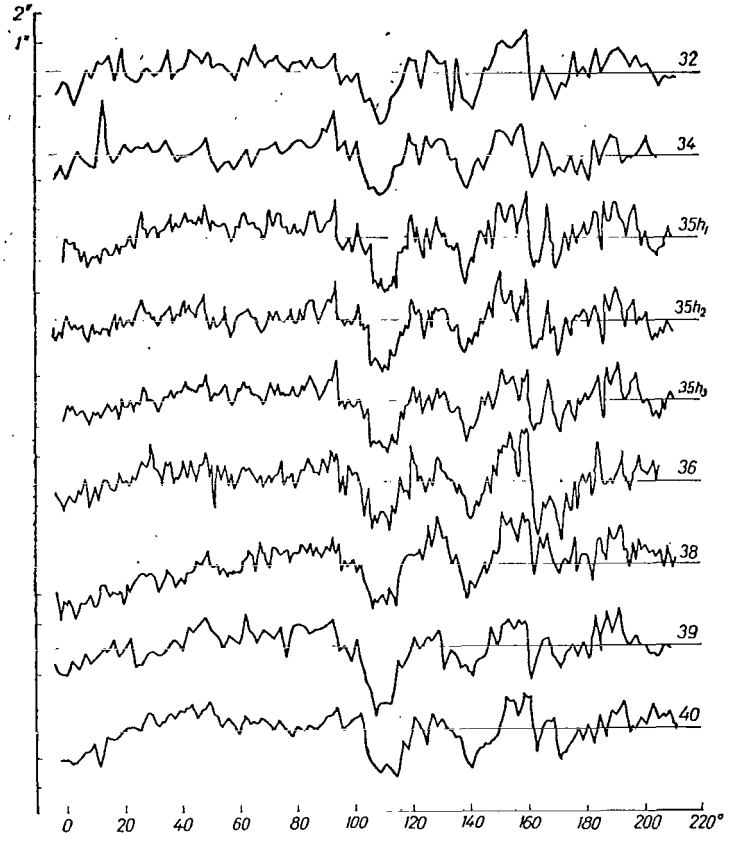

Fig. 9. Relief Altitudes of the Limb Zone (Plates).

Considering that the profiles obtained on the 12- and 10-meter coronagraphs subtend different sections of the lunar limb, a discrepancy would seem natural. To insure that all profiles were ultimately identical, on the plates and films we chose common 210° sections of the limb. For each photograph we solved system (9), then calculated ΔH_i in the 210° system and plotted these values on a graph. As before, the profiles of plates or films agree, but the plates do not coincide with the films. It also seems characteristic that the maximum difference in the altitudes is always observed at a position angle of 0 - 90°. Thus, either on the plates or on the films, the ring width was incorrectly formed in individual sections. The distortion of the profile may be attributed either to the solar limb or the lunar limb, or both together. Let us now attempt to determine whether the solar limb is actually its circumference. Let us first solve the system of boundary equations

/20

/21

$$\Delta x \cos P_i + \Delta y \sin P_i + R_0 = R_i, \qquad (11)$$

where R_i are the measured radius vectors of the Sun corrected for differential refraction. After correcting the radius vectors of the Sun, for the eccentricity of the artificial point we took the deviation $R_i - R_0 = \Delta R_i$ for each photograph individually. Analysis showed that for all plates, no significant systematic errors were detected in ΔR_i and, consequently, that the profiles of the limb zones were not subject to significant changes due to the small width of the ring. The deviations for the radius vectors of the Sun which

/22

we analyzed for the films indicates that ΔR_i does not contain systematic errors. The nature of these distortions is very difficult to explain in terms of known defects caused by the optics and technique of the observations. It is possible that the detected effect is a consequence of the red filter we used to photograph the annular solar eclipse. The red filter was placed in front of the cassette to obtain normal exposures, since it was not possible to increase the rotation rate of the shutter disk for unforeseen technical reasons. The expedition did not have a dark filter available, so we used a red filter since the chosen type of film has a 30% sensitivity in that region.

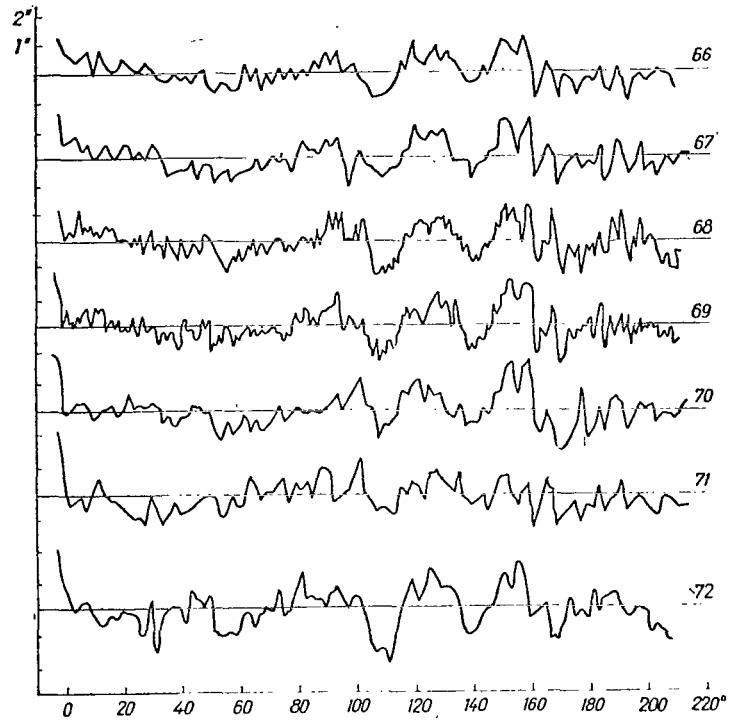

Fig. 10. Relief Altitudes of the Limb Zone (Films).

We introduced reductions into the measured radius vectors of the Sun and recalculated the ring width Δh_i and the relief altitudes of the Moon in the 210° system using (6)-(10). After plotting the obtained values of $\Delta H_i'$ on the graph and comparing these values with the profiles of the 12-meter coronagraph, no systematic difference was detected. Finally, our profiles were compared with the profile taken from the Watts map for the corresponding libration. No noticeable discrepancies were detected here either. The fine relief was equally well-described by the Watts profiles and the profiles obtained during the 1966 eclipse (Fig. 11). If there is some systematic difference, then firstly, it must be small and, secondly, we may

/23

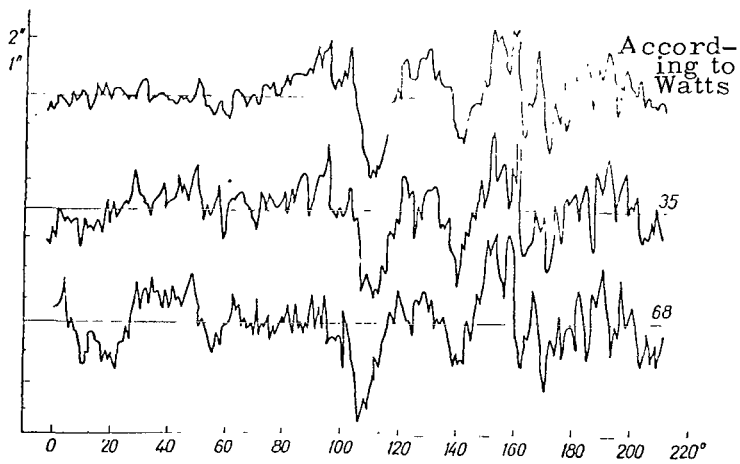

Fig. 11. Comparison of the Profiles Obtained During the Solar Eclipse of May 20, 1966 with the Watts Profiles.

attribute it to the fact that the centers of the probable circumferences from which we computed the altitudes on the Watts map and in our interpretations do not coincide. Thus, we may assume that systematic errors lie only in the solar radius vectors measured by the films. In our opinion, their source is the nonuniform brightness of the limb zones of the Sun in red flashes. Because of this problem, the limb does not appear to be smooth.

Based on this analysis, we may state that the measurements of the photographs of the annular eclipse of May 20, 1966 and the initial treatment of the data were conducted at a level sufficient that the results obtained may be successfully used to investigate the geometric shape of the lunar profile. In our investigation we used nine lunar profiles covering 265° and seven covering 255°, obtained on the 10- and 12-meter coronagraphs. Nine profiles describe the limb of the Moon in the region 310°-0°-210°; the remaining seven describe the limb in the region 356°-0°-247°. The section not covered by the measurements was the western limb. In our subsequent determination of the shape of the lunar profile, we used the measurements of the width of the 300° ring and the radius vectors of the points on the limb in this section, supplemented by measurements of the radius vectors of two crescents obtained a certain time after the third contact and subtending about 165° of the western limb of the Moon.

Reduction to a single system of radius vectors based on common sections was accompanied by a number of difficulties. Firstly, the photographic conditions were not identical; therefore, the density of the negatives differs. This fact led to nonuniform changes in the radius vectors due to photographic irradiation. Secondly, the photographs of the ring and the crescent were taken under different optical librations; therefore, the visibility conditions of a particular detail were not the same. Practically speaking, this difference is small and may be ignored. Thirdly, the influence of instrumental errors on the images is theoretically variable. Of the above-mentioned reductions, the most difficult to take into account is the effect of photographic irradiation. The action of irradiation on the image may lead to more drastic distortion of some sections of the relief and to less perceptible distortion of others. It is impossible to take into account changes of this type in the limb. If photographic irradiation decreases the radius vectors uniformly or its consequences follow a particular law (for example,

/24

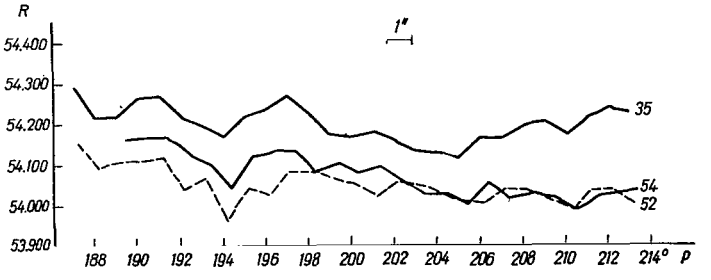

Fig. 12. Common Sections of the Limb of the Ring and the Crescents at Position Angles of 188-214°.

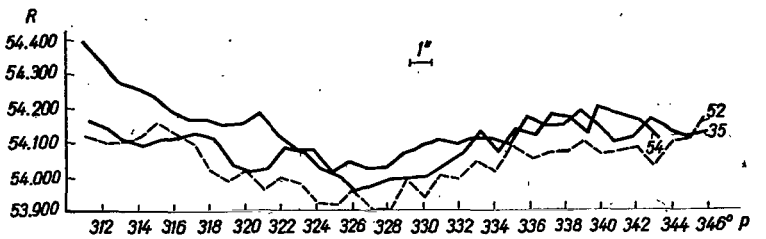

Fig. 13. Common Sections of the Limb of the Ring and the Crescents at Position Angles of 312-346°.

cosinusoidal), then with the corresponding method of reducing to a single coordinate system, the difference between two photographs caused by photographic irradiation may be ignored. From an analysis of the profiles of the ring, it follows that in the photographs of the 1966 eclipse there is no nonuniform action of irradiation on individual sections of the limb. The crescents have a comparatively large width, and the probability of this effect appearing are even less. Thus, the correct way to determine the profile of the Moon is to use radius vectors of the ring and the crescent simultaneously. /25

The radius vectors of the crescents were reduced to the system of the ring in the following way. First we found for the crescents R_i' corrected for the eccentricity of the marker and differential refraction. Then the radius vectors of the crescent and the ring were plotted on graphs for the common sections (Figs. 12, 13). The graphs show that the fine relief, within the margin of error of the measurements and computations, is represented identically by the crescent and the ring. However, the altitudes of limb points were computed from the probable circles whose centers do not coincide. Otherwise, either the curves would shift or the difference between the radius vectors would remain constant at all position angles. In Figure 14, let point A be a detail of the lunar limb. The altitude of point A above probable circle (1) is equal to AB, and its altitude above probable circle (2) is AC. The difference in altitudes $BC = CA - BA$ is caused by the fact that the centers of these circles do not coincide. By solving by least squares a system of conventional equations such as (9), where the free terms are taken from the graphs of $\Delta H_i = AB - AC$, we can find the rectangular coordinates of the origin of coordinates O' from its ratio to O. Using this system we can also reduce the radius of the crescent to the ring system of the 35th plate. To verify the correctness and efficiency of this method for reducing the radius vectors to a single system, the same

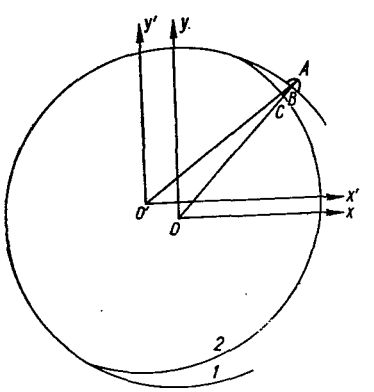

Fig. 14. Diagram of he Method for Reducing the Measurements of Two Photographs to a Single System.

operation was carried out on a model based on the fact that the centers of the probable circles do not coincide. They would coincide only if the lunar profile could be described by any curve but a circle. Such a curve might be an ellipse, for example. Therefore, on the ellipse we chose sections with arc lengths equal to the ring and the crescent (Figs. 15-17). We measured the radii of the conditional ring and crescent every 10°, reduced them to a single system and used them to obtain the parameters of the ellipse.

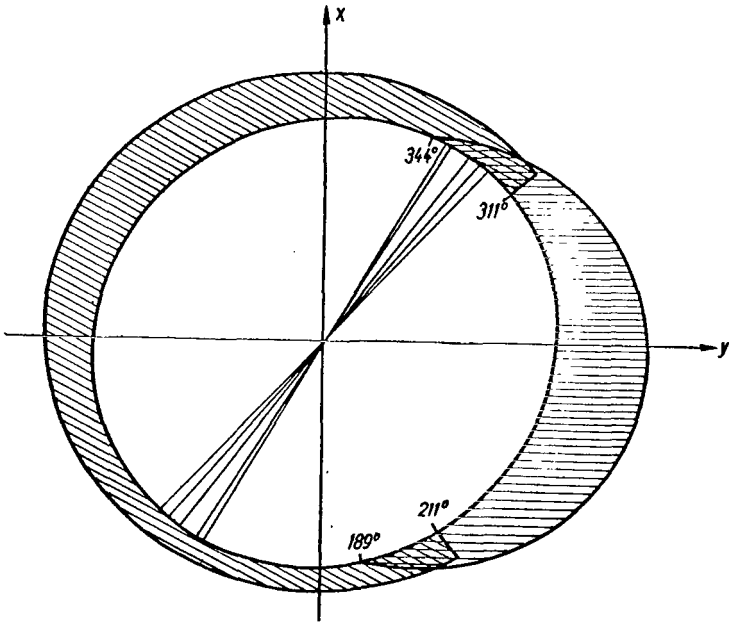

/26

Fig. 15. The "Ring-Crescent" Model.

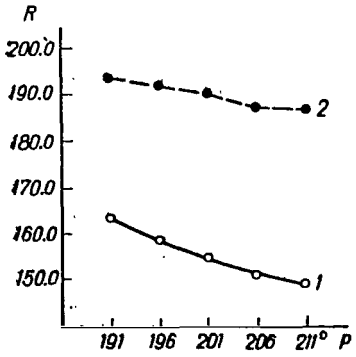

Fig. 16. Common Sections of the "Ring-Crescent" Model in Sections of 191-211°:
(1) "Ring"; (2) "Crescent".

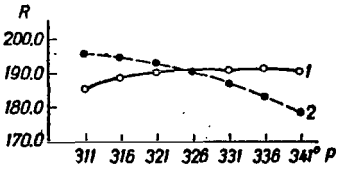

Fig. 17. Common Sections of the "Ring-Crescent" Model in Sections of 311-341°:
(1) "Ring"; (2) "Crescent".

The computed difference between the semiaxes and the direction of the major axis agree, within the margin of error, with the initial figures (Table 2). We should note here that according to the model, the radius of the probable circle of the crescent was larger than the radius obtained for the ring; when using the plates the situation was reversed. This fact may be used for interpretation of the shape of the lunar profile. /27

TABLE 2

Limb	e,mm	E
Total Disc (Initial)	41.5	-35.0°
Total Disc (After Reduction)	41.3	-34.7
East (0-180°).	42.6	-29.4
West (180-360°)	43.2	-29.0
North (270-90°)	41.4	-37.8
South (90-270°)	40.4	-40.4

Thus, our approach to determining the shape of the profile included both the measured width of the ring covering 300° and a single system of 976 radius vectors of the Moon (35th, 36th, 38th, 52nd and 54th plates) covering the entire limb at optical librations of $\lambda = 5.9°$, $\beta = -0.1°$.

Analysis of the Profiles and Conclusions

The geometric shape of the lunar profile may be determined in different ways. One of the methods consists in making an assumption (based on observational data) concerning the shape of the curve which best depicts the visible disc. Then the parameters can be determined from direct or indirect measurements. Using this method, in the past others have obtained for the profile a circle, an ellipse (Kh.I. Potter [6]) and several composite models (A.A. Yakovkin and A.A. Goryna [7]). Another approach involves direct analysis of the measurements. The results of these measurements allow us to choose a satisfactory curve in the best way. The latter method leads quickly and rationally to the desired result. An example of this approach is given in the paper by I.V. Gavrilov and A.N. Kur'yanova [12]. Based on the adjusted values of the irregularities for two profiles, I.V. Gavrilova and A.N. Kur'yanova reached the conclusion that ellipticity was not a characteristic of the shape of the lunar disc. The authors of [5] also conducted a harmonic analysis of measurements of the ring widths, but the profile shape could not be described by any particular curve.

In this article we will present analytically radius vectors and altitudes obtained from our observations of the annular eclipse /28

on May 20, 1966 as a Fourier series:

$$F(P_i) = F_0 + k_1 \sin P_i + k_2 \cos P_i + k_3 \sin 2P_i + k_4 \cos 2P_i + \\ + k_5 \sin 3P_i + k_6 \cos 3P_i + k_7 \sin 4P_i + k_8 \cos 4P_i, \quad (12)$$

where $F(P_i)$ is the radius vector of R_i or the altitude $\Delta H_i'$ of the limb point for position angle P_i.

The solution to conventional equations such as (12) provides the following expressions for the lunar profile: according to the radius vectors of the total disc (35th, 36th, 38th, 52nd and 54th plates)

$$R = R_0 - 0.36'' \sin P - 0.17'' \cos P + \\ 0.59'' \sin 2P - 0.33'' \cos 2P + \\ 0.29'' \sin 3P - 0.06'' \cos 3P - \\ 0.22'' \sin 4P - 0.06'' \cos 4P ; \quad (13)$$

and according to the ring width extending 311°-0°-247° (the 35th [measured three times], 36th and 38th plates and the 68th and 69th films)

$$\Delta H' = \Delta H_0 - 0.58'' \sin P - 0.61'' \cos P + \\ 0.62'' \sin 2P - 1.11'' \cos 2P + \\ 1.08'' \sin 3P - 0.34'' \cos 3P - \\ 0.07'' \sin 4P + 0.53'' \cos 4P . \quad (14)$$

The 36th, 38th and 52nd plates were assigned a weight of 1; the 35th and 54th plates were assigned a weight of 3. The weights were assigned in direct proportion to the number of times each point was used in the measurements.

To compare the results obtained with similar results, let us now introduce the expansions for zero libration borrowed from [5]. These expansions were derived on the basis of photographs of the annular eclipse of 1963 and the charts of the limb zone of the Moon compiled by Watts:

$$R = R_0 - 0.21'' \sin P - 0.11'' \cos P + \\ + 0.54'' \sin 2P - 0.16'' \cos 2P + \\ + 0.27'' \sin 3P - 0.05'' \cos 3P - \\ - 0.16'' \sin 4P + 0.11'' \cos 4P , \quad (15)$$

$$R = R_0 - 0.32'' \sin P - 0.16'' \cos P + \\ + 0.59'' \sin 2P - 0.21'' \cos 2P + \\ + 0.27'' \sin 3P - 0.05'' \cos 3P - \\ - 0.32'' \sin 4P + 0.21'' \cos 4P . \quad (16)$$

It follows from (13), (15) and (16) that the corresponding coefficients for the sines and cosines are reasonably consistent: i.e., the profile can be presented as an expansion of the altitude into a Fourier series. The coefficients in (14) are noticeably /29

different from their counterparts in (13), (15) and (16), since they were obtained using an incomplete profile. Based on (13)-(16), the Hine profile at zero libration, the A.A. Yakovkin shape from [12] and Kh.I. Potter's ellipse, we can compute the elliptical components; i.e., the difference between the semiaxes e and the direction of the major axis E (Table 3).

TABLE 3

Data Used	e	E	Libration λ	Libration β
Profile According to Yakovkin	0.68″	-20°	0 ;	0
Photographs of the Full Moon (Kh.I. Potter)	0.76	-36	2.5;	-1.4
Hine Chart	1.0	-23	0 ;	0
Watts Chart	1.25	-35	0 ;	0
Annular Eclipse of 1963	1.13	-37	0 ;	0
Annular Eclipse of 1966	1.35	-31	-5.9;	-0.1

It follows from the table that only the first two values of e differ significantly from the others. Considering that the Yakovkin profile is not the result of direct measurements and that Potter's results were obtained from photographs taken when the Moon was on the wane, the inconsistency would seem to be natural. The other results agree satisfactorily with each other and yield a single value for the prolation of the Moon in a north-northwest direction, which is confirmed by extensive known observational data. However, the concept that the profile of the Moon is an ellipse is explained in (13)-(16) only by the terms with sin $2P$, cos $2P$, sin $4P$, cos $4P$, etc. The other coefficients are also significant in terms of absolute value and, within the margin of error of the calculations, agree with independent observations. This situation forces us to seek to describe the lunar profile by a curve which can explain the presence of coefficients of all orders in (12). Such a curve is a limacon of Pascal; i.e., conchoid of a circle. In canonical form, its equation is

$$(x^2+y^2-ax)^2=l^2(x^2+y^2), \tag{17}$$

in parametric form it is

$$\begin{aligned} x&=a\cos^2\varphi+l\cos\varphi,\\ y&=a\cos\varphi\sin\varphi+l\sin\varphi, \end{aligned} \tag{18}$$

and in polar coordinates it is

$$r = a\cos\varphi + l. \tag{19}$$

We can now show that in the measurement coordinate system the radius vector R can be described by an expression such as (12). It follows from Figure 18 that

$$R^2 = r^2 + \sigma^2 - 2r\sigma\cos\gamma, \tag{20}$$

where

$$\gamma = P - \alpha - x.$$

It is easy to show that the angle x is small for the Moon. With sufficient accuracy we may say that

$$\begin{aligned} \gamma &= P - \alpha, \\ \varphi &= P - \alpha + \beta = P - \varphi_0. \end{aligned} \tag{21}$$

Thus

$$R^2 = [a\cos(P - \varphi_0) + l]^2 + \sigma^2 - 2\sigma[a\cos(P - \varphi_0) + l]\cos(P - \alpha)$$

or

$$\begin{aligned} R = l\Bigg[1 + \frac{\sigma^2}{l^2} + \frac{\frac{1}{2}a^2 - a\sigma\cos(\varphi_0 - \alpha)}{l^2} - \frac{2a\sin\varphi_0}{l}\sin P + \\ + \frac{2a\cos\varphi_0}{l}\cos P + \frac{\frac{1}{2}a^2\cos 2\varphi_0 - a\sigma\cos\varphi_0\cos\alpha}{l^2}\cos 2P + \\ + \frac{\frac{1}{2}a_2\sin 2\varphi_0 + a\sigma\sin(\alpha - \varphi_0)}{l^2}\sin 2P + \ldots\Bigg]^{\frac{1}{2}}. \end{aligned} \tag{22}$$

By expanding (22) into a series, we find that

$$\begin{aligned} R = F_0 &+ A_1\sin P + B_1\cos P + \\ &+ A_2\sin 2P + B_2\cos 2P + \\ &+ A_3\sin 3P + B_3\cos 3P + \\ &+ A_4\sin 4P + B_4\cos 4P + \ldots; \end{aligned} \tag{23}$$

where

$$F_0,\ A_l,\ B_l = f(a,\ \sigma,\ l,\ \alpha,\ \beta).$$

According to the values of the coefficients in (13)-(16), it /31
is easy to determine that, in our case, $a < 1$. We can determine the parameters of the most probable limacon according to the measurements. To do this we will use rectangular coordinates for the limb points ξ and η obtained for the profile at zero libration using the Watts charts [5]. After performing simple transformations and solving conditional equations such as (18), we obtain

$$a = 0.42''; \quad \alpha = 55^\circ.$$

The angle α between the abscissa of the limacon and the axis of rotation of the Moon is computed from the north through the east (Fig. 19). The direction of prolation and the value of a are confirmed by the data of Table 3.

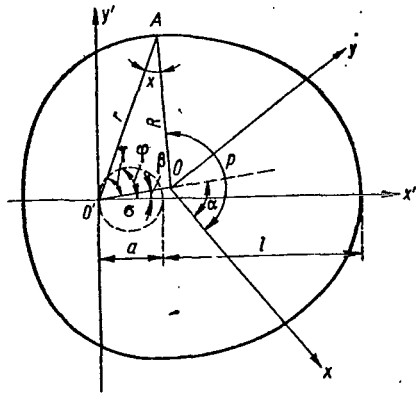

Fig. 18.

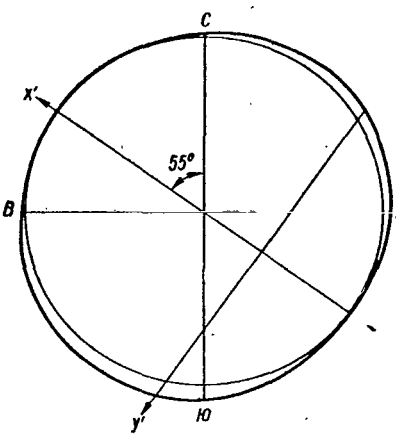

Fig. 19.

Fig. 18. Limacon of Pascal.

Fig. 19. Profile of the Moon as a Limacon of Pascal. The Discrepancy Between the Limacon and the Circle Has Been Exaggerated Approximately 100 Times.

We can now use the limacon of Pascal to explain some known observational effects. Let us now enumerate them.

(a) Width corrections, obtained strictly from observations of occultations (eastern limb) and emersion (western edge), are systematically different. Including a small number of emersions along with the occultations in the investigation always decreases the absolute value of the negative correction for width b_0. According to Spencer-Jones [9], for occultations $b_0 = -0.61''$ and for emersions $b_0 = -0.28''$.

(b) The observations show that passing through the half-moon /32

phase, the correction for the tabular longitude of the moon undergoes a discontinuity. The difference in the longitudes computed separately according to the eastern and western limbs reaches 1.2".

(c) The inclinations of the lunar orbit, computed separately from observations of the northern and eastern limbs, do not coincide. The difference $\Delta i_S - \Delta i_N$ is always positive.

(d) The curvatures of the eastern and western limbs are different. All series of heliometric and photographic observations yield a higher value for the radius of the eastern limb of the Moon than for the western limb with average optical libration over width. For example, I.V. Bel'kovich's article [10] presents the following differences in radius (east minus west):

Hartwig I	+0.18"
Hartwig II	+0.04"
Banakhevich	+0.22"
Yakovkin	+0.11"
Bel'kovich	+0.14"
Average	+0.14 ± 0.03" mean error

(e) We discovered from observations of star occultations that generally the northeastern part of the Moon is lower than a certain mean level. As a result emersions are delayed. This is substantiated by measurements of the radius vectors of this part of the profile.

(f) The centers of the probable circles determined using half the disc, whose center shifts along the circle, can be described by a hypocycloid [6].

TABLE 4

Limb (180°)	Δx mm	Δy mm	R, mm
Eastern	-1.3	+ 9.0	166.0
Western	+0.6	-10.9	165.2
Northern	+9.5	+ 0.8	169.6
Southern	-9.1	- 1.4	166.4

TABLE 5

Limb (180°)	Δx mm	Δy mm	R, mm
Eastern	-0.7	-0.5	14.7
Western	+0.3	+0.2	14.2
Northern	-1.2	-0.6	15.1
Southern	-1.0	+0.5	13.9

These and other observed facts can be explained by our proposed model of the profile. To facilitate matters, interpretations of the cited contradictions are given in Tables 4 and 5, which include the results of solutions to the systems of conventional equations /33 such as (11) for the northern, eastern, southern and western sections of the lunar profile. As baseline data we used the values of R_i taken from the curves plotted on an arbitrary scale. Some of the indicated contradictions can be adequately explained by an ellipse (Table 4) and the limacon of Pascal (Table 5). However, the

presence of significant coefficients for the terms sin P, cos P, sin $3P$ and cos $3P$ in expansions (13)-(16) cannot be explained by the elliptical model. According to this model, these terms in the expansion would have to be so small as to be negligible.

It follows from what we have said that the overall shape of the lunar profile is best described by a limacon of Pascal. The parameters given above for the limacon were calculated for a specific case. With other librations the parameters will probably differ from the real ones. The values of a and α undoubtedly show a relationship to the optical libration, but the data available to us in this investigation are insufficient to determine the libration effect.

Finally, it is interesting to compare the geometric shape of the lunar profile with the gravitational shape. To do this, we borrowed from [8] a curve for the level of the gravitational potential of the Moon in the plane of the figure $\lambda = 90°$. We used the radius vectors of the surface cross section of the level, measured every 10° according to the position angle, to expand into a Fourier series using (12):

$$\begin{aligned} r = r_0 &+0.07'' \sin \beta - 0.06'' \cos \beta + \\ &+0.03'' \sin 2\beta - 0.02'' \cos 2\beta - \\ &-0.09'' \sin 3\beta - 0.04'' \cos 3\beta - \\ &-0.12'' \sin 4\beta - 0.06'' \cos 4\beta + \\ &+0.11'' \sin 5\beta - 0.02'' \cos 5\beta - \\ &-0.04'' \sin 6\beta + 0.02'' \cos 6\beta - \\ &-0.07'' \sin 7\beta + 0.01'' \cos 7\beta - \\ &-0.14'' \sin 8\beta - 0.13'' \cos 8\beta - \\ &-0.02'' \sin 9\beta + 0.01'' \cos 9\beta - \\ &-0.08'' \sin 10\beta + 0.02'' \cos 10\beta - \\ &-0.07'' \sin 11\beta + 0.08'' \cos 11\beta - \\ &-0.07'' \sin 12\beta - 0.17'' \cos 12\beta + \ldots \end{aligned} \qquad (24)$$

Equation (24) contains some high-order terms, since these terms are not always small. In contrast to the coordinate system used before, here we will use a right-handed selenocentric system. All the coefficients in (24) only slightly exceed the calculation /34
errors in terms of absolute value. Therefore, it is inadvisable to draw any conclusions or to make any computations on the basis of (24). Nevertheless, we should note that the equipotential curve and the limacon of Pascal which describes the lunar profile have a certain similarity. On both curves, the curvature of the western limb is slightly larger than that of the eastern limb. However, the directions of prolation of the limacon and the potential levels do not coincide. It may be that this is the result of the presence of isostacy on the Moon.

The proposed curve has three parameters and tends to level off the fine relief of the lunar profile rather drastically. Therefore, it is interesting to derive a characteristic for the deviation of

of individual details. To do this we computed the mean square error of "one detail" for all photographs of the 1966 annular eclipse. This characteristic was equal to 0.80". Based on this calculation, we computed mean square errors for our calculation of the coefficients in (13). None of them exceeded ±0.03".

Thus, according to observations of the two annular solar eclipses of 1963 and 1966, according to photographs of the full Moon slightly on the wane, according to the Watts charts compiled using a large number of observations of various limb sections and according to other recent observational data, we determined unique values for the dimensions and direction of prolation of the lunar profile. Thus, instead of a circle we have proposed two plane figures, an ellipse and a limacon of Pascal, which best equalize the fine relief. Representing the profile as a circle cannot cope with a number of significant contradictions of an observed nature. The elliptical model exhibits fewer contradictions with the observations, but all the same it cannot explain the terms of odd-numbered order when the radius vectors are expanded into a Fourier series. The limacon of Pascal best fits the observations and explains the contradictions known at this time. When applied to the Moon, all three curves have a small number of parameters. Naturally, there is a large number of plane figures with a large number of parameters which can more successfully level off the fine relief. However, the more complex the curve, the more difficult it is to use in practice in order to determine the coordinates of the Moon. It is also difficult to relate a complex geometric shape to the gravitational figure, the progressive motion or the rotational motion of the Moon.

The problem of determining the coordinates of the Moon has not been finally resolved, since at the present time the parameters of the proposed curves have been determined with certainty only for particular librations. In addition, we do not yet have a method /35
for determining the coordinates of the center of mass from observations. It is advisable to solve the problem in the following way. First, we must determine from observations the position of the point which is fixed on the disc of a certain geometric figure for concrete values of libration. Then we must find a method for converting from this point to the center of mass of the Moon. In this case, we may use any of the existing detailed charts of the relief of the limb zone and any plane curve which levels off the relief of the profile.

References

1. Vasilenko, N.A.: Determining the Coordinates of the Site and the Moments of the Annular Solar Eclipse of May 20, 1966 (cf. this issue).
2. Skorik, K.Ye.: Description of the High-Speed Cassette and Shutter for Observing the Annular Eclipse of May 20, 1966 (cf. this issue).
3. Plyugin, G.A.: Bull. of the Main Astronomical Observ. of the Acad of Sci., USSR, Vol. 22, No. 1, p. 166, 1960.
4. Weimer, T.: Atlas de profiles lunaires (Atlas of Lunar Profiles). Paris, 1952.
5. Carson, D. and M. Davidson: Icarus, New York-London, Vol. 5, No. 4, 1966.
6. Potter, Kh.I. and N.F. Bystrov: Astronomicheskiy zhurnal, Vol. 38, No. 5, 1961.
7. Yakovkin, A.A. and A.A. Gorynya: In the Collection: Trudy 14-y astronomicheskoy konferentsii SSSR (Proceedings of the 14th Astronomical Converence of the USSR). Moscow-Leningrad, Academy of Sciences of the USSR Press, 1960.
8. Akim, E.L.: In the Collection: Kosmicheskiye Issledovaniya (Space Exploration). Moscow, "Nauka" Press, Ch. 4, p. 6, 1966.
9. Spencer-Jones, H.: Monthly Notices, Vol. 90, No. 71, 1952.
10. Bel'kovich, I.V.: Izvestiya astronomicheskoy observatorii imeni V.P. Engel'garta, Kazan', Vol. 109, No. 2, p. 24, 1949.
11. Yakovkin, A.A.: Astron. zhurnal, Vol. 39, No. 4, 1962.
12. Gavrilov, I.V. and A.N. Kur'yanova: In the Collection: Voprosy Astrometrii (Problems of Astrometry). Kiev, "Naukova Dumka" Press, 1964.

TABLE 1

P	$R_{\mathbb{C}}$	$R_{\odot}$	P	$R_{\mathbb{C}}$	$R_{\odot}$
		Plate No. 32			
213.8	54.190	—	125.8	.944	.676
211.8	.192	54.486	123.8	.844	.705
209.8	.174	.483	121.8	.947	.719
207.8	.114	.433	119.8	.946	.718
205.8	.077	.442	117.8	.912	.744
203.8	.108	.453	115.8	.868	.754
201.8	.165	.484	113.8	.793	.727
199.8	.118	.454	111.8	.748	.758
197.8	.142	.453	109.8	.735	.771
195.8	.110	.480	107.8	.752	.749
193.8	.038	.495	105.8	.787	.731
191.8	.167	.496	103.8	.812	.767
189.8	.154	.505	101.8	.919	.769
187.8	.111	.514	99.8	.854	.743
185.7	.018	.483	97.8	.911	.778
183.8	54.132	.520	95.8	.858	.760
181.8	53.982	.486	93.8	.974	.760
179.8	54.037	.521	91.8	.944	.768
177.8	.012	.532	89.8	.954	.782
175.8	54.055	.515	87.8	.959	.788
173.8	53.924	.523	85.8	.975	.765
171.8	.960	.558	83.8	.966	.788
169.8	.881	.541	81.8	.973	.769
167.8	.968	.575	79.8	.978	.772
165.8	.972	.545	77.8	.979	.800
163.8	.968	.611	75.8	53.970	.770
161.8	53.849	.579	73.8	54.017	.773
159.8	54.082	.561	71.8	54.033	.798
157.8	54.019	.556	69.8	53.996	.781
155.8	53.945	.522	67.8	54.032	.780
153.8	.987	.572	65.8	.062	.750
151.8	.998	.573	63.8	.036	.786
149.8	.983	.580	61.8	.054	.777
147.8	.914	.604	59.8	.000	.791
145.8	.862	.567	57.8	.025	.783
143.8	.859	.627	55.8	.034	.763
141.8	.794	.670	53.8	.044	.751
139.8	.764	.620	51.8	.022	.727
137.8	.789	.641	49.8	.105	.750
135.8	.912	.629	47.8	.100	.774
133.8	.873	.688	45.8	.123	.755
131.8	.908	.651	43.8	.163	.763
129.8	.917	.677	41.8	.160	.818
127.8	.921	.655	39.8	.136	.787

TABLE 1 (cont.)

P	$R_{\mathbb{C}}$	$R_{\odot}$	P	$R_{\mathbb{C}}$	$R_{\odot}$
37.8	.157	.821	357.8	.328	.771
35.8	.219	.769	355.8	.335	.781
33.8	.171	.789	353.8	.366	.775
31.8	.180	.794	351.8	.344	.806
29.8	.239	.815	349.8	.368	.758
27.8	.281	.847	347.8	.319	.757
25.8	.246	.843	345.8	.314	.794
23.8	.225	.798	343.8	.354	.800
21.8	.281	.828	341.8	.375	.793
19.8	.350	.788	339.8	.407	.769
17.8	.288	.825	337.8	.373	.769
15.8	.354	.787	335.8	.359	.767
13.8	.367	.817	333.8	.381	.772
11.8	.352	.784	331.8	.339	.741
9.8	.323	.791	329.8	.311	.727
7.8	.342	.774	327.8	.275	.706
5.8	.326	.818	325.8	.293	.719
3.8	.297	.824	323.8	.319	.735
1.8	.353	.794	321.8	.397	.745
359.8	.368	.786	319.8	54.337	54.752
		Plate No. 34			
311.8	54.382	—	359.8	.103	.598
313.8	.238	—	1.8	.066	.630
315.8	.191	54.553	3.8	.077	.592
317.8	.114	.553	5.8	.111	.592
319.8	.058	.548	7.8	.089	.611
321.8	.092	.553	9.8	.044	.594
323.8	54.020	.547	11.8	.039	.603
325.8	53.982	.566	13.8	.295	.629
327.8	54.018	.565	15.8	.073	.587
329.8	.014	.533	17.8	.024	.602
331.8	.015	.528	19.8	.056	.614
333.8	.092	.568	21.8	.076	.606
335.8	.128	.551	23.8	.063	.632
337.8	.184	.583	25.8	.052	.614
339.8	.171	.564	27.8	.052	.626
341.8	.143	.559	29.8	.047	.620
343.8	.135	.574	31.8	.020	.635
345.8	.070	.590	33.8	.020	.642
347.8	.076	.608	35.8	.047	.638
349.8	.126	.617	37.8	54.011	.641
351.8	.090	.587	39.8	53.987	.672
353.8	.088	.615	41.8	54.009	.687
355.8	.091	.619	43.8	.029	.710
357.8	.086	.621	45.8	.016	.700

P	$R_{\mathbb{C}}$	$R_{\odot}$	P	$R_{\mathbb{C}}$	$R_{\odot}$
47.8	.044	.717	131.8	.153	.929
49.8	54.064	.713	133.8	.091	.930
51.8	53.994	.730	135.8	.098	.923
53.8	53.950	.737	137.8	.032	.947
55.8	54.000	.769	139.8	.010	.938
57.8	53.962	.734	141.8	.087	.931
59.8	.954	.761	143.8	.068	.874
61.8	53.976	.745	145.8	.068	.910
63.8	54.006	.754	147.8	.140	.906
65.8	53.959	.776	149.8	.210	.894
67.8	54.014	.776	151.8	.218	.894
69.8	53.998	.764	153.8	.213	.893
71.8	54.025	.794	155.8	.134	.851
73.8	.038	.792	157.8	.234	.871
75.8	.020	.816	159.8	.249	.870
77.8	.025	.822	161.8	.036	.847
79.8	.051	.823	163.8	.086	.852
81.8	.087	.853	165.8	.165	.829
83.8	.072	.858	167.8	.146	.826
85.8	.060	.857	169.8	.053	.812
87.8	.061	.857	171.8	.098	.818
89.8	.115	.855	173.8	.071	.797
91.8	.094	.846	175.8	.139	.800
93.8	.162	.842	177.8	.062	.779
95.8	.022	.856	179.8	.108	.766
97.8	.057	.855	181.8	.049	.765
99.8	.002	.873	183.8	.186	.753
101.8	54.080	.878	185.8	.086	.727
103.8	53.992	.881	187.8	.171	.736
105.8	.913	.889	189.8	.195	.707
107.8	.926	.896	191.8	.204	.716
109.8	.904	.897	193.8	.094	.689
111.8	.902	.884	195.8	.131	.691
113.8	53.942	.883	197.8	.160	.708
115.8	54.020	.899	199.8	.137	.654
117.8	.025	.901	201.8	.192	.651
119.8	.156	.919	203.8	.137	.640
121.8	.104	.905	205.8	.134	.647
123.8	.039	.916	207.8	.122	.611
125.8	.146	.914	209.8	.119	.582
127.8	.112	.916	211.8	.159	54.585
129.8	.149	.928	213.8	54.170	—
		Plate No. 35			
311	54.391	54.641	313	.250	.609
312	.327	.617	314	.221	.620

/39 /38

TABLE 1 (cont.)

P	$R_{\mathbb{C}}$	$R_{\odot}$	P	$R_{\mathbb{C}}$	$R_{\odot}$	P	$R_{\mathbb{C}}$	$R_{\odot}$	P	$R_{\mathbb{C}}$	$R_{\odot}$
315	.185	.583	2	.641	.068	49	.568	.002	96	.691	.357
316	.136	.592	3	.634	.065	50	.513	.010	97	.705	.389
317	.094	.536	4	.646	.082	51	.471	54.018	98	.729	.392
318	.084	.528	5	.603	.055	52	.483	53.999	99	.747	.412
319	.057	.525	6	.583	.046	53	.488	54.023	100	.701	.395
320	.048	.512	7	.586	.038	54	.508	.048	101	.757	.431
321	54.068	.501	8	.537	.036	55	.487	.021	102	.804	.432
322	53.999	.497	9	.551	.058	56	.526	.036	103	.749	.428
323	.946	.494	10	.562	.028	57	.509	.075	104	.720	.435
324	.934	.445	11	.556	.039	58	.467	.066	105	.752	.445
325	.856	.436	12	.580	.051	59	.459	.053	106	.651	.480
326	.872	.401	13	.576	.075	60	.524	.065	107	.653	.466
327	.844	.383	14	.596	.066	61	.541	.084	108	.673	.504
328	.831	.412	15	.577	.040	62	.558	.076	109	.703	.524
329	.865	.376	16	.557	.044	63	.568	.092	110	.689	.544
330	.876	.370	17	.547	.031	64	.576	.110	111	.701	.547
331	.881	.358	18	.547	.000	65	.539	.097	112	.690	.542
332	.860	.392	19	.532	.032	66	.556	.114	113	.762	.562
333	.867	.348	20	.567	.025	67	.541	.116	114	.783	.611
334	.853	.295	21	.544	.024	68	.548	.137	115	.839	.656
335	.824	.259	22	.565	.039	69	.535	.152	116	.926	.649
336	.893	.303	23	.548	.007	70	.559	.158	117	.903	.636
337	.860	.301	24	.547	.042	71	.632	.165	118	.953	.655
338	.849	.292	25	.543	.024	72	.603	.168	119	53.942	.648
339	.881	.291	26	.568	54.016	73	.600	.188	120	54.057	.674
340	.830	.280	27	.584	53.985	74	.605	.153	121	.064	.672
341	.774	.272	28	.565	54.001	75	.601	.193	122	.041	.719
342	.780	.265	29	.552	.017	76	.586	.178	123	.093	.717
343	.821	.279	30	.555	.020	77	.598	.203	124	.026	.765
344	.776	.262	31	.545	.015	78	.602	.206	125	.037	.759
345	.750	.269	32	.542	.019	79	.661	.239	126	.145	.788
346	.754	.246	33	.509	.021	80	.649	.263	127	.103	.812
347	.721	.235	34	.532	.012	81	.638	.258	128	.182	.831
348	.731	.201	35	.531	.008	82	.659	.244	129	.194	.816
349	.735	.222	36	.527	.001	83	.663	.276	130	.198	.849
350	.735	.222	37	.567	.013	84	.696	.274	131	.222	.873
351	.710	.206	38	.523	.017	85	.698	.247	132	.196	.844
352	.684	.186	39	.522	54.003	86	.725	.283	133	.166	.873
353	.714	.202	40	.513	53.994	87	.717	.279	134	.185	.896
354	.672	.166	41	.525	54.007	88	.670	.319	135	.179	.895
355	.657	.143	42	.550	53.986	89	.723	.342	136	.197	.894
356	.637	.141	43	.528	54.003	90	.728	.336	137	.146	.896
357	.646	.106	44	.509	53.984	91	.764	.345	138	.134	.911
358	.632	.090	45	.507	53.995	92	.768	.349	139	.096	.931
359	.656	092	46	.517	54.016	93	.749	.330	140	.142	.906
0	.622	.095	47	.515	53.988	94	.837	.342	141	.172	.930
1	.682	.087	48	.526	54.011	95	.701	.365	142	.214	.961

/141 /140

TABLE 1 (cont.)

P	$R_{\mathbb{C}}$	$R_{\odot}$	P	$R_{\mathbb{C}}$	$R_{\odot}$	P	$R_{\mathbb{C}}$	$R_{\odot}$	P	$R_{\mathbb{C}}$	$R_{\odot}$
143	.239	.955	179	.619	.205	201	.130	.703	154	.896	.411
144	.278	.924	180	.636	.199	200	.147	.665	153	.794	.416
145	.297	.965	181	.601	.211	199	.156	.676	152	.880	.433
146	.293	.964	182	.656	.226	198	.239	.675	151	.820	.414
147	.319	.933	183	.733	.269	197	.179	.688	150	.806	.422
148	.295	.982	184	.725	.235	196	.158	.668	149	.772	.426
149	.352	.996	185	.676	.250	195	.091	.636	148	.778	.413
150	.451	54.996	186	.616	.279	194	.197	.622	147	.703	.407
151	.483	55.005	187	.790	.258	193	.062	.605	146	.701	.407
152	.446	.035	188	.724	.252	192	.069	.622	145	.719	.411
153	.440	.039	189	.730	.262	191	.144	.634	144	.724	.362
154	.455	.038	190	.783	.253	190	.193	.593	143	.790	.393
155	.425	.035	191	.792	.240	189	54.107	.578	142	.818	.392
156	.465	.041	192	.748	.247	188	53.995	.594	141	.779	.380
157	.418	.069	193	.727	.267	187	54.045	.559	140	.826	.389
158	.497	.069	194	.700	.271	186	.044	.599	139	.808	.364
159	.539	.117	195	.754	.268	185	54.032	.551	138	.813	.368
160	.582	.083	196	.783	.275	184	53.992	.546	137	.855	.383
161	.373	.080	197	.821	.280	183	53.903	.565	136	.832	.358
162	.345	.090	198	.781	.308	182	54.023	.577	135	.882	.359
163	.396	.123	199	.730	.279	181	53.924	.567	134	.854	.337
164	.381	.103	200	.727	.284	180	.925	.588	133	.795	.362
165	.441	.142	201	.745	.277	179	.938	.537	132	.813	.360
166	.519	.143	202	.722	.292	178	.888	.584	131	.728	.330
167	.596	.135	203	.704	.302	177	.825	.595	130	.746	.334
168	.516	.162	204	.700	.289	176	.846	.541	129	.791	.330
169	.472	.132	205	.693	.291	175	.918	.564	128	.775	.335
170	.416	.157	206	.740	.288	174	.954	.581	127	.802	.300
171	.428	.168	207	.744	.313	173	.940	.554	126	.872	.293
172	.517	.183	208	.773	.293	172	.900	.559	125	.724	.344
173	.561	.177	209	.786	.295	171	.915	.550	124	.754	.338
174	.568	.193	210	.759	55.298	170	.893	.590	123	.715	.306
175	.519	.190	211	.799	—	169	.822	.583	122	.760	.302
176	.605	.183	212	.826	—	168	.834	.552	121	.671	.300
177	.568	.177	213	54.819	—	167	53.978	.544	120	.642	.311
178	.583	.192				166	54.158	.528	119	.649	.292
		Plate No. 36				165	.107	.499	118	.582	.313
						164	54.113	.490	117	.584	.262
219	54.309	54.742	210	.195	.709	163	53.968	.510	116	.594	.255
218	.300	.749	209	.253	.702	162	53.972	.517	115	.589	.250
217	.263	.751	208	.247	.721	161	54.022	.474	114	.601	.299
216	.259	.720	207	.196	.698	160	.061	.444	113	.621	.289
215	.258	.730	206	.209	.697	159	.001	.440	112	.551	.268
214	.253	.744	205	.216	.703	158	.036	.472	111	.711	.281
213	.249	.736	204	.264	.702	157	54.009	.472	110	.664	.270
212	.249	.705	203	.229	.698	156	53.974	.425	109	.626	.296
211	.243	.709	202	.192	.698	155	.878	.432	108	.732	.275

/43 /42

TABLE 1 (cont.)

P	$R_{\mathbb{C}}$	$R_{\odot}$	P	$R_{\mathbb{C}}$	$R_{\odot}$	P	$R_{\mathbb{C}}$	$R_{\odot}$	P	$R_{\mathbb{C}}$	$R_{\odot}$
107	.722	.234	60	.869	.332	13	.227	.607	344	.421	.830
106	.703	.218	59	.921	.322	12	.174	.611	343	.487	.828
105	.723	.233	58	.779	.342	11	.206	.622	342	.378	.853
104	.747	.220	57	.939	.333	10	.188	.644	341	.417	.840
103	.688	.269	56	.923	.356	9	.202	.662	340	.398	.813
102	.710	.230	55	.958	.306	8	.232	.668	339	.381	.859
101	.698	.266	54	.927	.317	7	.256	.703	338	.444	.827
100	.835	.261	53	.961	.351	6	.191	.673	337	.381	.844
99	.783	.252	52	.942	.393	5	.225	.682	336	.390	.864
98	.816	.231	51	.951	.380	4	.228	.668	335	.367	.865
97	.767	.258	50	.980	.351	3	.274	.690	334	.415	.872
96	.814	.268	49	.941	.370	2	.244	.692	333	.370	.907
95	.822	.263	48	.949	.349	1	.282	.710	332	.397	.897
94	.800	.293	47	.972	.338	0	.293	.714	331	.369	.902
93	.797	.271	46	.942	.366	359	.286	.733	330	.389	.896
92	.808	.287	45	.940	.362	358	.310	.724	329	.418	.907
91	.814	.269	44	.944	.380	357	.315	.730	328	.465	.915
90	.816	.249	43	.990	.349	356	.329	719	327	.450	.951
89	.801	.276	42	53.990	.363	355	.320	.729	326	.463	.938
88	.834	.304	41	54.022	.378	354	.310	.745	325	.463	.942
87	.809	.294	40	53.966	.403	353	.297	.744	324	.472	.936
86	.783	.319	39	54.013	.402	352	.348	.753	323	.511	.929
85	.819	.293	38	54.012	.386	351	.355	.748	322	.576	955
84	.798	.283	37	53.990	.360	350	.377	.766	321	.588	.952
83	.817	.304	36	54.099	.384	349	.343	.768	320	.628	.931
82	.787	.302	35	.036	.410	348	.308	.804	319	.653	.943
81	.828	.249	34	.051	.412	347	.360	.784	318	.711	.951
80	.808	.280	33	.035	.383	346	.402	.797	317	.766	.945
79	.835	.310	32	.052	.424	345	.397	.811	316	54.776	54.938
78	.815	.314	31	.046	.448						
77	.834	.306	30	.054	.447						
76	.825	.314	29	.029	.456			Plate No. 38			
75	.806	.321	28	.066	.468						
74	.833	.300	27	.049	.462	310.6	54.478	54.882	324.6	.125	.842
73	.818	.302	26	.055	.467	311.6	.418	.922	325.6	.108	.841
72	.814	.285	25	.107	.479	312.6	.371	.923	326.6	.101	.809
71	.852	.292	24	.074	.504	313.6	.343	.927	327.6	.107	.802
70	.850	.282	23	.064	.493	314.6	.365	.898	328.6	.156	.808
69	.856	.300	22	.106	.524	315.6	.328	.895	329.6	.180	.784
68	.836	.267	21	.117	.514	316.6	.324	.846	330.6	.195	.808
67	.878	.322	20	.162	.550	317.6	.256	.863	331.6	.170	.783
66	.853	.333	19	.140	.552	318.6	.219	.883	332.6	.279	.799
65	.809	.306	18	.111	.581	319.6	.230	.842	333.6	.204	.776
64	.885	.327	17	.144	.555	320.6	.178	.845	334.6	.235	.780
63	.833	.318	16	.102	.556	321.6	.179	.828	335.6	.217	.793
62	.885	.293	15	.109	.592	322.6	.217	.840	336.6	.246	.769
61	.861	.297	14	.206	.598	323.6	.160	.832	337.6	.314	.776

TABLE 1 (cont.)

P	$R_{\mathbb{C}}$	$R_{\odot}$	P	$R_{\mathbb{C}}$	$R_{\odot}$	P	$R_{\mathbb{C}}$	$R_{\odot}$	P	$R_{\mathbb{C}}$	$R_{\odot}$
338.6	.241	.772	25.6	.040	.405	72.6	54.001	.336	119.6	54.037	.524
339.6	.294	.752	26.6	.042	.396	73.6	53.999	.347	120.6	.010	.504
340.6	.284	.724	27.6	.057	.412	74.6	.988	.350	121.6	.024	.514
341.6	.237	.723	28.6	.050	.417	75.6	.986	.347	122.6	.014	.538
342.6	.131	.705	29.6	.046	.404	76.6	.993	.346	123.6	.033	.549
343.6	.187	.714	30.6	.041	.394	77.6	.991	.391	124.6	.056	.522
344.6	.216	.716	31.6	54.002	.379	78.6	53.988	.358	125.6	.113	.512
345.6	.223	.702	32.6	53.972	.401	79.6	54.021	.388	126.6	.051	.539
346.6	.201	.668	33.6	.992	.402	80.6	.012	.382	127.6	.098	.526
347.6	.126	.668	34.6	53.998	.390	81.6	.035	.384	128.6	.161	.531
348.6	.177	.661	35.6	54.012	.352	82.6	.042	.402	129.6	.119	.533
349.6	.172	.645	36.6	.009	.371	83.6	.005	.390	130.6	.054	.509
350.6	.155	.632	37.6	54.004	.376	84.6	.028	.380	131.6	.082	.543
351.6	.163	.605	38.6	53.962	.373	85.6	.017	.411	132.6	.048	.541
352.6	.133	.603	39.6	53.991	.387	86.6	.021	.386	133.6	.000	.556
353.6	.130	.598	40.6	54.001	.385	87.6	54.003	.388	134.6	.037	.567
354.6	.118	.611	41.6	53.981	.391	88.6	53.994	.403	135.6	54.013	.551
355.6	.125	.576	42.6	54.013	.377	89.6	54.029	.414	136.6	53.990	.559
356.6	.113	.591	43.6	54.003	.374	90.6	.057	.431	137.6	.912	.568
357.6	.129	.555	44.6	53.999	.366	91.6	.014	.418	138.6	.884	.579
358.6	.112	.566	45.6	54.009	.338	92.6	.071	.420	139.6	.929	.568
359.6	.108	.567	46.6	.007	.340	93.6	.008	.418	140.6	.914	.561
360.6	.079	.556	47.6	.040	.384	94.6	54.050	.427	141.6	.902	.568
1.6	.119	.573	48.6	.027	.354	95.6	53.956	.427	142.6	.950	.574
2.6	.087	.572	49.6	54.051	.352	96.6	.986	.428	143.6	.966	.570
3.6	.085	.600	50.6	53.991	.342	97.6	53.973	.441	144.6	.988	.565
4.6	.073	.580	51.6	.981	.343	98.6	—	—	145.6	.975	.599
5.6	.107	.564	52.6	.968	.325	99.6	54.015	.472	146.6	53.988	.594
6.6	.109	.568	53.6	.937	.328	100.6	53.966	.462	147.6	54.052	.600
7.6	.102	.558	54.6	.963	.330	101.6	54.008	.481	148.6	.023	.579
8.6	.113	.547	55.6	.984	.360	102.6	53.977	.487	149.6	.040	.593
9.6	.091	.528	56.6	.962	.361	103.6	.933	.482	150.6	.174	.588
10.6	.062	.536	57.6	.950	.344	104.6	.898	.487	151.6	.159	.614
11.6	.059	.516	58.6	.954	.332	105.6	.849	.496	152.6	.134	.595
12.6	.105	.499	59.6	.940	.323	106.6	.863	.474	153.6	.156	.591
13.6	.108	.500	60.6	.951	.348	107.6	.850	.476	154.6	.143	.623
14.6	.122	.516	61.6	.977	.334	108.6	.861	.476	155.6	.140	.638
15.6	.086	.517	62.6	53.981	.329	109.6	.860	.470	156.6	.100	.631
16.6	.085	.506	63.6	54.002	.326	110.6	.836	.480	157.6	.201	.628
17.6	.082	.501	64.6	53.981	.316	111.6	.873	.465	158.6	.155	.620
18.6	.040	.489	65.6	.941	.349	112.6	.874	.494	159.6	.202	.650
19.6	.059	.474	66.6	.991	.337	113.6	.859	.492	160.6	54.145	.607
20.6	.026	.485	67.6	.990	.324	114.6	.839	.503	161.6	53.954	.607
21.6	.051	.445	68.6	.973	.314	115.6	53.971	.502	162.6	53.939	.579
22.6	.037	.453	69.6	.960	.336	116.6	54.001	.524	163.6	54.081	.596
23.6	.018	.413	70.6	.948	.347	117.6	53.988	.484	164.6	.018	.574
24.6	.025	.407	71.6	53.983	.311	118.6	53.994	.481	165.6	.056	.626

TABLE 1 (cont.)

P	$R_{\mathbb{C}}$	$R_{\odot}$	P	$R_{\mathbb{C}}$	$R_{\odot}$	P	$R_{\mathbb{C}}$	$R_{\odot}$	P	$R_{\mathbb{C}}$	$R_{\odot}$
166.6	.118	.626	191.6	.252	.752	137.4	.319	.850	43.4	.809	.031
167.6	.079	.661	192.6	.143	.737	135.4	.378	.850	41.4	.735	.034
168.6	54.047	.652	193.6	.148	.738	133.4	.418	.876	39.4	.741	.009
169.6	53.998	.634	194.6	.084	.738	131.4	.368	.888	37.4	.766	.038
170.6	53.982	.652	195.6	.181	.751	129.4	.494	.866	35.4	.713	.022
171.6	54.020	.638	196.6	.150	.779	127.4	.502	.898	33.4	.708	.028
172.6	.051	.658	197.6	.231	.777	125.4	.529	.916	31.4	.721	.028
173.6	.041	.670	198.6	.194	.789	123.4	.509	.922	29.4	.711	.028
174.6	.091	.698	199.6	.197	.771	121.4	.572	.955	27.4	.684	55.047
175.6	.161	.700	200.6	.209	.792	119.4	.542	54.974	25.4	.630	54.996
176.6	.044	.701	201.6	.211	.815	117.4	.544	55.012	23.4	.671	.943
177.6	.095	.696	202.6	.202	.806	115.4	.582	.036	21.4	.624	.940
178.6	.120	.722	203.6	.200	.814	113.4	.477	.074	19.4	.578	.916
179.6	.112	.712	204.6	.227	.816	111.4	.499	.083	17.4	.618	.900
180.6	.089	.690	205.6	.207	.831	109.4	.511	.096	15.4	.573	.899
181.6	.038	.737	206.6	.194	.842	107.4	.480	.096	13.4	.570	.895
182.6	.137	.746	207.6	.231	.815	105.4	.599	.097	11.4	.530	.883
183.6	.182	.730	208.6	.235	.849	103.4	.638	.071	9.4	.514	.897
184.6	.170	.718	209.6	.214	.864	101.4	.769	.104	7.4	.503	.851
185.6	.100	.702	210.6	.189	.837	99.4	.700	.109	5.4	.453	.859
186.6	.098	.728	211.6	.224	.855	97.4	.743	.093	3.4	.468	.850
187.6	.210	.724	212.6	.232	.845	95.4	.735	.098	1.4	.418	.851
188.6	.199	.744	213.6	.220	54.795	93.4	.818	.069	359.4	.388	.822
189.6	.180	.737	214.6	54.208	—	91.4	.848	.112	357.4	.372	.773
190.6	.219	.739				89.4	.846	.118	355.4	.379	.805
						87.4	.840	.118	353.4	.324	.809
		Plate No. 39				85.4	.808	.086	351.4	.325	.777
						83.4	.865	.116	349.4	.257	.799
213.4	53.650	—	175.4	.971	.515	81.4	.876	.115	347.4	.219	.751
211.4	.604	—	173.4	.947	.516	79.4	.864	.111	345.4	.241	.727
209.4	.637	54.239	171.4	.908	.525	77.4	.763	.113	343.4	.225	.701
207.4	.648	.240	169.4	53.961	.543	75.4	.888	.124	341.4	.214	.702
205.4	.623	.255	167.4	54.072	.572	73.4	.871	.141	339.4	.147	.719
203.4	.599	.221	165.4	.058	.562	71.4	.883	.139	337.4	.120	.685
201.4	.708	.306	163.4	.086	.637	69.4	.860	.097	335.4	.077	.657
199.4	.732	.302	161.4	.015	.643	67.4	.807	.091	333.4	54.087	.654
197.4	.775	.329	159.4	.300	.669	65.4	.831	.080	331.4	53.987	.652
195.4	.740	.321	157.4	.315	.677	63.4	.905	.079	329.4	.867	.632
193.4	.779	.317	155.4	.252	.691	61.4	.790	.068	327.4	.867	.610
191.4	.881	.327	153.4	.326	.722	59.4	.777	.047	325.4	.880	.582
189.4	.844	.374	151.4	.334	.751	57.4	.797	.048	323.4	.956	.571
187.4	.899	.349	149.4	.274	.750	55.4	.763	.058	321.4	.870	.563
185.4	.814	.400	147.4	.345	.761	53.4	.781	.037	319.4	.855	.556
183.4	.915	.370	145.4	.292	.799	51.4	.783	.010	317.4	.902	.546
181.4	.846	.450	143.4	.277	.786	49.4	.859	.036	315.4	53.994	54.482
179.4	.913	.456	141.4	.232	.804	47.4	.834	.039	313.4	54.020	—
177.4	.872	.463	139.4	.282	.808	45.4	.785	.015			

TABLE 1 (cont.)

P	$R_{\mathbb{C}}$	$R_{\odot}$	P	$R_{\mathbb{C}}$	$R_{\odot}$
		Plate No. 40			
209.5	53.947	54.582	117.5	53.982	.434
207.5	.974	.554	115.5	.999	.415
205.5	.949	.539	113.5	.869	.415
203.5	.927	.519	111.5	.903	.411
201.5	.962	.507	109.5	.943	.429
199.5	.899	.508	107.5	.918	.421
197.5	.915	.502	105.5	.951	.436
195.5	.918	.530	103.5	53.996	.418
193.5	.909	.533	101.5	54.129	.404
191.5	.986	.501	99.5	.128	.409
189.5	.927	.484	97.5	.150	.451
187.5	.944	.484	95.5	.123	.443
185.5	.842	.469	93.5	.220	.461
183.5	.919	.468	91.5	.216	.468
181.5	.812	.449	89.5	.228	.485
179.5	.840	.409	87.5	.169	.457
177.5	.824	.438	85.5	.174	.462
175.5	.865	.425	83.5	.224	.507
173.5	.785	.391	81.5	.216	.503
171.5	.749	.391	79.5	.229	.502
169.5	.769	.424	77.5	.200	.505
167.5	.898	.407	75.5	.250	.536
165.5	.883	.392	73.5	.310	.547
163.5	.849	.389	71.5	.288	.558
161.5	.783	.393	69.5	.318	.561
159.5	53.985	.388	67.5	.368	.593
157.5	54.009	.395	65.5	.345	.582
155.5	53.924	.388	63.5	.367	.605
153.5	53.966	.368	61.5	.389	.601
151.5	54.000	.381	59.5	.348	.620
149.5	53.956	.424	57.5	.382	.621
147.5	.888	.398	55.5	.446	.658
145.5	.862	.391	53.5	.400	.643
143.5	.877	.397	51.5	.452	.651
141.5	.875	.412	49.5	.502	.656
139.5	.811	.408	47.5	.492	.671
137.5	.855	.420	45.5	.456	.665
135.5	53.972	.445	43.5	.498	.668
133.5	54.006	.462	41.5	.500	.676
131.5	.037	.464	39.5	.500	.688
129.5	.074	.463	37.5	.493	.707
127.5	.069	.465	35.5	.515	.712
125.5	54.123	.475	33.5	.479	.710
123.5	53.981	.442	31.5	.476	.716
121.5	54.058	.437	29.5	.501	.702
119.5	54.100	.442	27.5	.518	.724
25.5	.499	.773	347.5	.422	.916
23.5	.509	.772	345.5	.415	.939
21.5	.538	.801	343.5	.393	.918
19.5	.553	.815	341.5	.447	.917
17.5	.504	.807	339.5	.400	.932
15.5	.493	.809	337.5	.407	.910
13.5	.523	.837	335.5	.368	.932
11.5	.426	.848	333.5	.414	.940
9.5	.483	.832	331.5	.286	.942
7.5	.514	.891	329.5	.250	.930
5.5	.471	.861	327.5	.240	.938
3.5	.454	.884	325.5	.245	.961
1.5	.446	.878	323.5	.311	.950
359.5	.451	.883	321.5	.282	.964
357.5	.457	.897	319.5	.265	.980
355.5	.452	.887	317.5	.369	.998
353.5	.421	.940	315.5	.385	54.989
351.5	.446	.902	313.5	.489	—
349.5	.440	.905	311.5	54.608	—
			Film No. 66		
238.2	45.591	45.858	188.2	.431	.996
236.2	.632	.823	186.2	.414	.983
234.2	.615	.799	184.2	.479	45.985
232.2	.576	.840	182.2	.442	46.008
230.2	.582	.837	180.2	.425	45.991
228.2	.562	.857	178.2	.408	.992
226.2	.541	.866	176.2	.331	.977
224.2	.568	.878	174.2	.363	.958
222.2	.568	.878	172.2	.316	.908
220.2	.545	.884	170.2	.233	.918
218.2	.483	.902	168.2	.298	.908
216.2	.552	.844	166.2	.300	.884
214.2	.508	.884	164.2	.186	.859
212.2	.492	.871	162.2	.114	.845
210.2	.449	.890	160.2	.253	.834
208.2	.473	.879	158.2	.307	.836
206.2	.488	.888	156.2	.225	.837
204.2	.511	.915	154.2	.219	.822
202.2	.498	.938	152.2	.263	.842
200.2	.465	.929	150.2	.252	.839
198.2	.520	.972	148.2	.180	.841
196.2	.512	45.987	146.2	.139	.860
194.2	.442	46.010	144.2	.146	.858
192.2	.492	46.010	142.2	.119	.886
190.2	.521	45.997	140.2	.079	.865

/50 /51

TABLE 1 (cont.)

P	$R_{\mathbb{C}}$	$R_{\odot}$	P	$R_{\mathbb{C}}$	$R_{\odot}$	P	$R_{\mathbb{C}}$	$R_{\odot}$	P	$R_{\mathbb{C}}$	$R_{\odot}$
138.2	.088	.877	66.2	.198	.007	201.9	.641	.116	105.9	.546	.338
136.2	.162	.910	64.2	.174	.019	199.9	.613	.119	103.9	.550	.329
134.2	.186	.920	62.2	.240	.019	197.9	.683	.097	101.9	.606	.340
132.2	.206	.914	60.2	.159	46.021	195.9	.641	.141	99.9	.568	.333
130.2	.199	.943	58.2	.134	45.994	193.9	.637	.178	97.9	.548	.409
128.2	.281	.973	56.2	.186	46.022	191.9	.708	.183	95.9	.514	.272
126.2	.254	.993	54.2	.217	.036	189.9	.750	.191	93.9	.564	.248
124.2	.214	45.987	52.2	.221	.067	187.9	.678	.218	91.9	.532	.251
122.2	.237	46.002	50.2	.268	.091	185.9	.617	.255	89.9	.519	.211
120.2	.277	45.984	48.2	.320	.072	183.9	.760	.245	87.9	.456	.194
118.2	.196	46.001	46.2	.314	.066	181.9	.648	.212	85.9	.438	.162
116.2	.228	.010	44.2	.292	.070	179.9	.683	.239	83.9	.452	.170
114.2	.184	.039	42.2	.307	.060	177.9	45.615	46.210	81.9	.450	.140
112.2	.122	46.019	40.2	.302	.057	175.9	.683	.234	79.9	.420	.156
110.2	.082	45.994	38.2	.329	.052	173.9	.636	.258	77.9	.371	.163
108.2	.079	46.004	36.2	.334	.077	171.9	.645	.250	75.9	.400	.142
106.2	.050	45.979	34.2	.381	.105	169.9	.590	.274	73.9	.417	.169
104.2	.091	.980	32.2	.386	.098	167.9	.667	.253	71.9	.429	.156
102.2	.106	.970	30.2	.413	.082	165.9	.706	.265	69.9	.405	.157
100.2	.106	.930	28.2	.455	.093	163.9	.633	.266	67.9	45.356	46.124
98.2	.104	.940	26.2	.424	.085	161.9	.591	.282	65.9	.389	.112
96.2	.110	.960	24.2	.416	.065	159.9	.779	.262	63.9	.386	.144
94.2	.179	.959	22.2	.453	.064	157.9	.756	.293	61.9	.381	.140
92.2	.148	.970	20.2	.498	.083	155.9	.678	.302	59.9	.365	.124
90.2	.181	.961	18.2	.468	.080	153.9	.751	.290	57.9	.350	.130
88.2	.123	.958	16.2	.448	.051	151.9	.760	.275	55.9	.371	.109
86.2	.112	.926	14.2	.467	.037	149.9	.747	.281	53.9	.365	.112
84.2	.128	.979	12.2	.515	.031	147.9	.649	.284	51.9	.350	.121
82.2	.133	45.975	10.2	.485	.063	145.9	.631	.284	49.9	.414	.116
80.2	.129	46.000	8.2	.561	.047	143.9	.621	.310	47.9	.429	.120
78.2	.149	45.983	6.2	.584	.087	141.9	.598	.311	45.9	.376	.114
76.2	.130	.994	4.2	.609	.118	139.9	.533	.298	43.9	.428	.094
74.2	.139	.966	2.2	.661	.133	137.9	.571	.276	41.9	.383	.077
72.2	.129	45.999	0.2	.699	.148	135.9	.600	.310	39.9	.397	.079
70.2	.168	46.002	358.2	45.791	46.176	133.9	.602	.320	37.9	.400	.091
68.2	.139	.027				131.9	.646	.314	35.9	.400	.094
		Film No. 67				129.9	.684	.304	33.9	.414	.061
						127.9	.676	.322	31.9	45.421	46.007
237.9	45.786	45.975	219.9	.646	.079	125.9	.712	.346	29.9	.452	.007
235.9	.729	46.030	217.9	.689	.086	123.9	45.656	46.326	27.9	.420	46.014
233.9	.738	.007	215.9	.710	.064	121.9	.672	.332	25.9	.409	45.976
231.9	.720	.017	213.9	.678	.066	119.9	.696	.324	23.9	.413	.999
229.9	.737	.048	211.9	.635	.030	117.9	.623	.336	21.9	.418	.944
227.9	.708	.006	209.9	.623	.072	115.9	.604	.332	19.9	.475	45.991
225.9	.676	.018	207.9	.658	.085	113.9	.564	.345	17.9	.445	46.001
223.9	.689	.045	205.9	.637	.071	111.9	.565	.359	15.9	.469	45.993
221.9	.673	.059	203.9	.589	.102	109.9	.555	.373	13.9	.486	.976

TABLE 1 (cont.)

P	$R_{\mathbb{C}}$	$R_{\odot}$	P	$R_{\mathbb{C}}$	$R_{\odot}$	P	$R_{\mathbb{C}}$	$R_{\odot}$	P	$R_{\mathbb{C}}$	$R_{\odot}$
11.9	.458	.972	3.9	.498	.920	79.7	.142	.824	126.7	.498	.078
9.9	.437	.955	1.9	.508	.931	80.7	.162	.821	127.7	.502	.074
7.9	.482	.943	359.9	.521	947	81.7	.190	.836	128.7	.524	.097
5.9	.459	.935	357.9	45.584	45.895	82.7	.172	.828	129.7	.522	.087
		Film No. 68				83.7	.144	.815	130.7	.502	.109
						84.7	.170	.828	131.7	.533	.110
357.7	45.287	45.637	38.7	.087	.730	85.7	.163	.854	132.7	.498	.126
358.7	.248	.653	39.7	.116	.695	86.7	.183	.811	133.7	.514	.134
359.7	.196	.648	40.7	.086	.696	87.7	.164	.849	134.7	.516	.142
0.7	.210	.643	41.7	.085	.730	88.7	.185	.840	135.7	.528	.154
1.7	.210	.640	42.7	.112	.741	89.7	.208	.846	136.7	.519	.195
2.7	.200	.647	43.7	.096	.704	90.7	.260	.830	137.7	.511	.165
3.7	.202	.624	44.7	.088	.704	91.7	.185	.814	138.7	.479	.169
4.7	.249	.613	45.7	.095	.734	92.7	.240	.819	139.7	.478	.189
5.7	.155	.597	46.7	.093	.730	93.7	.211	.838	140.7	.498	.187
6.7	.168	.596	47.7	.139	.717	94.7	.289	.856	141.7	.498	.204
7.7	.140	.593	48.7	.144	.724	95.7	.198	.878	142.7	.559	.227
8.7	.132	.566	49.7	.134	.738	96.7	.210	.877	143.7	.579	.215
9.7	.089	.551	50.7	.094	.722	97.7	.221	.890	144.7	.557	.214
10.7	.068	.528	51.7	.061	.719	98.7	.225	.891	145.7	.582	.208
11.7	.064	.543	52.7	.066	.734	99.7	.282	.898	146.7	.608	.228
12.7	.080	.542	53.7	.049	.738	100.7	.185	.853	147.7	.656	.223
13.7	.108	.553	54.7	.020	.723	101.7	.284	.882	148.7	.646	.219
14.7	.104	.569	55.7	.017	.748	102.7	.269	.882	149.7	.709	.220
15.7	.087	.547	56.7	.043	.743	103.7	.229	.912	150.7	.776	.254
16.7	.074	.547	57.7	.050	.725	104.7	.223	.936	151.7	.756	.294
17.7	.045	.555	58.7	.033	.724	105.7	.130	.916	152.7	.780	.294
18.7	.059	.570	59.7	.067	.725	106.7	.145	.932	153.7	.803	.298
19.7	.034	.550	60.7	.074	.771	107.7	.164	.953	154.7	.787	.272
20.7	.047	.575	61.7	.085	.784	108.7	.184	.946	155.7	.744	.279
21.7	.025	.553	62.7	.132	.754	109.7	.178	.968	156.7	.717	.322
22.7	.012	.563	63.7	.102	.765	110.7	.228	45.989	157.7	.819	.298
23.7	.054	.573	64.7	.114	.753	111.7	.239	46.012	158.7	.833	.302
24.7	.054	.603	65.7	.083	.750	112.7	.289	.020	159.7	.824	.304
25.7	.090	.604	66.7	.102	.755	113.7	.277	.020	160.7	.680	.291
26.7	.051	.636	67.7	.097	.754	114.7	.334	.035	161.7	.622	.281
27.7	.088	.646	68.7	.096	.770	115.7	.353	.028	162.7	.629	.286
28.7	.108	.636	69.7	.076	.767	116.7	.392	.035	163.7	.692	.280
29.7	.150	.662	70.7	.085	.762	117.7	.405	.058	164.7	.687	.278
30.7	.092	.675	71.7	.103	.758	118.7	.400	.049	165.7	.705	.298
31.7	.123	.692	72.7	.119	.753	119.7	.453	.055	166.7	.837	.298
32.7	.126	.705	73.7	.108	.752	120.7	.459	.055	167.7	.749	.278
33.7	.096	.723	74.7	.133	.785	121.7	.442	.027	168.7	.730	.296
34.7	.146	.689	75.7	.095	.787	122.7	.435	.035	169.7	.673	.314
35.7	.112	.673	76.7	.123	.799	123.7	.437	.038	170.7	.635	.315
36.7	.115	.702	77.7	.112	.792	124.7	.440	.074	171.7	.729	.330
37.7	.105	.720	78.7	.130	.826	125.7	.480	.082	172.7	.733	.305

/54
/55

TABLE 1 (cont.)

P	$R_{\mathbb{C}}$	$R_{\odot}$	P	$R_{\mathbb{C}}$	$R_{\odot}$	P	$R_{\mathbb{C}}$	$R_{\odot}$	P	$R_{\mathbb{C}}$	$R_{\odot}$
173.7	.733	.334	209.7	.794	.341	229.4	.607	.150	182.4	.126	.717
174.7	.712	.315	210.7	.849	.325	228.4	.612	.138	181.4	.072	.700
175.7	.794	.356	211.7	.832	.318	227.4	.587	.125	180.4	.133	.678
176.7	.716	.369	212.7	.842	.302	226.4	.583	.097	179.4	.113	.689
177.7	.757	.351	213.7	.848	.284	225.4	.574	.131	178.4	.092	.673
178.7	.784	.331	214.7	.858	.295	224.4	.591	.132	177.4	.073	.673
179.7	.789	.362	215.7	.863	.302	223.4	.581	.090	176.4	.087	.678
180.7	.794	.337	216.7	.870	.290	222.4	.593	.115	175.4	.038	.669
181.7	.756	344	217.7	.801	.267	221.4	.541	.119	174.4	.036	.660
182.7	.864	.365	218.7	.824	.304	220.4	.502	.080	173.4	.061	.658
183.7	.850	.359	219.7	.836	.287	219.4	.478	.074	172.4	45.013	.643
184.7	.775	.338	220.7	.859	.301	218.4	.501	.085	171.4	44.954	.661
185.7	.761	.322	221.7	.884	.323	217.4	.539	.098	170.4	.918	.642
186.7	.870	.337	222.7	.861	.320	216.4	.526	.083	169.4	44.982	.646
187.7	.881	.321	223.7	.872	.327	215.4	.509	.080	168.4	45.036	.623
188.7	.867	.338	224.7	.876	.318	214.4	.499	.065	167.4	.088	.610
189.7	.859	.357	225.7	.852	.333	213.4	.472	.051	166.4	45.010	.601
190.7	.930	.323	226.7	.889	.316	212.4	.486	.004	165.4	44.954	.593
191.7	.874	.331	227.7	.909	.293	211.4	.448	.024	164.4	.939	.559
192.7	.860	.372	228.7	.873	.295	210.4	.429	.018	163.4	.979	.589
193.7	.788	.360	229.7	.879	.290	209.4	.427	46.032	162.4	.878	.574
194.7	.846	.330	230.7	.865	.274	208.4	.433	45.978	161.4	44.909	.553
195.7	.822	.336	231.7	.838	.270	207.4	.412	.993	160.4	45.060	.532
196.7	.929	.336	232.7	.856	.265	206.4	.410	.989	159.4	.083	.537
197.7	.870	.350	233.7	.902	.256	205.4	.397	.973	158.4	.066	.520
198.7	.852	.344	234.7	.833	.246	204.4	.365	.958	157.4	45.029	.487
199.7	.866	.341	235.7	.868	.235	203.4	.382	.931	156.4	44.996	.512
200.7	.865	.313	236.7	.840	.214	202.4	.382	.939	155.4	45.020	.532
201.7	.858	.323	237.7	.858	.238	201.4	.348	.886	154.4	.027	.521
202.7	.837	.332	238.7	.954	.239	200.4	.330	.889	153.4	.066	.517
203.7	.816	.327	239.7	.908	.274	199.4	.315	.863	152.4	.072	.516
204.7	.793	334	240.7	.903	.250	198.4	.302	.880	151.4	.048	.543
205.7	.839	.346	241.7	.888	.263	197.4	.349	.876	150.4	45.061	.556
206.7	.835	.341	242.7	.866	.232	196.4	.275	.865	149.4	44.997	.544
207.7	.802	.347	243.7	45.857	46.204	195.4	.293	.857	148.4	.956	.529
208.7	.840	.323				194.4	.194	.822	147.4	.992	.535
						193.4	.278	.798	146.4	.913	.536
		Film No. 69				192.4	.206	.791	145.4	.942	.558
						191.4	.287	.812	144.4	.906	.562
245.4	45.816	46.139	237.4	.640	.145	190.4	.242	.794	143.4	.895	.561
244.4	.820	.171	236.4	.652	.144	189.4	.187	.786	142.4	.908	.568
243.4	.815	.193	235.4	.645	.161	188.4	.168	.758	141.4	.898	.596
242.4	.824	.209	234.4	.656	.154	187.4	.248	.782	140.4	.895	.581
241.4	.817	.162	233.4	.649	.137	186.4	.123	.760	139.4	.872	.577
240.4	.793	.170	232.4	.619	.156	185.4	.126	.778	138.4	.871	.560
239.4	.734	.188	231.4	.638	.149	184.4	.208	.702	137.4	.912	.542
238.4	.728	.160	230.4	.658	.135	183.4	.214	.723	136.4	.948	.563

/56
/57

TABLE 1 (cont.)

P	$R_{\mathbb{C}}$	$R_{\odot}$	P	$R_{\mathbb{C}}$	$R_{\odot}$	P	$R_{\mathbb{C}}$	$R_{\odot}$	P	$R_{\mathbb{C}}$	$R_{\odot}$
41.4	.374	.927	18.4	.716	.244	135.4	.963	.565	88.4	.063	.635
40.4	.312	.969	17.4	.712	.268	134.4	.983	.513	87.4	.024	.652
39.4	.324	.988	16.4	.752	.279	133.4	.937	.556	86.4	.039	.655
38.4	.351	.990	15.4	.763	.295	132.4	.936	.512	85.4	.062	.655
37.4	.400	45.999	14.4	.758	.312	131.4	.987	.522	84.4	.048	.664
36.4	.415	46.013	13.4	.816	.302	130.4	.967	.526	83.4	.085	.648
35.4	.418	.039	12.4	.834	.313	129.4	44.999	.506	82.4	.085	.643
34.4	.453	.045	11.4	.816	.307	128.4	45.017	.517	81.4	.068	.682
33.4	.459	.065	10.4	.813	.289	127.4	44.986	.513	80.4	.058	.647
32.4	.451	.084	9.4	.805	.338	126.4	.980	.523	79.4	.074	.650
31.4	.513	.093	8.4	.851	.352	125.4	.976	.547	78.4	.072	.684
30.4	.557	.125	7.4	.861	.334	124.4	.918	.520	77.4	.031	.686
29.4	.550	.121	6.4	.862	.345	123.4	.872	.494	76.4	.034	.676
28.4	.571	.150	5.4	.837	.352	122.4	.881	.489	75.4	.020	.690
27.4	.606	.177	4.4	.873	.378	121.4	.873	466	74.4	.045	.684
26.4	.642	.166	3.4	.820	.345	120.4	.942	.510	73.4	.051	.690
25.4	.591	.188	2.4	.840	.355	119.4	.896	.473	72.4	.077	.691
24.4	.613	.187	1.4	.856	.363	118.4	.888	.491	71.4	.102	.723
23.4	.638	.159	0.4	.902	.376	117.4	.906	.470	70.4	.085	.719
22.4	.634	.206	359.4	.870	.390	116.4	.885	.476	69.4	.074	.710
21.4	.651	.215	358.4	45.946	.355	115.4	.873	.498	68.4	.086	.706
20.4	.664	.236	357.4	46.029	.407	114.4	.854	.517	67.4	.080	.722
19.4	.678	.243	356.4	46.086	46.415	113.4	.803	.510	66.4	.079	.718
						112.4	.834	.520	65.4	.106	.728
		Film No. 70				111.4	.818	.501	64.4	.084	.729
						110.4	.801	.529	63.4	.123	.734
247.7	46.074	46.714	205.7	46.006	.987	109.4	.821	.541	62.4	.130	.745
245.7	.092	.758	203.7	45.981	.988	108.4	.809	.559	61.4	.114	.741
243.7	46.001	.803	201.7	46.021	.964	107.4	.831	.516	60.4	.110	.758
241.7	45.960	.815	199.7	45.993	.944	106.4	.788	.528	59.4	.123	.771
239.7	46.019	.831	197.7	46.038	.970	105.4	.803	.514	58.4	.112	.775
237.7	45.940	.877	195.7	45.978	.966	104.4	.895	.553	57.4	.149	.785
235.7	.913	.862	193.7	45.944	.965	103.4	.874	.536	56.4	.169	.782
233.7	.915	.863	191.7	46.024	.941	102.4	.938	.543	55.4	.198	.796
231.7	.928	.902	189.7	.034	.928	101.4	.952	.596	54.4	.166	.828
229.7	.952	.883	187.7	46.002	.900	100.4	.954	.581	53.4	.177	.810
227.7	.942	.891	185.7	45.874	.883	99.4	.944	.562	52.4	.178	.836
225.7	.930	.902	183.7	.946	.864	98.4	.950	.555	51.4	.190	.844
223.7	.929	.889	181.7	.854	.851	97.4	.957	.550	50.4	.147	.829
221.7	.973	.902	179.7	.857	.853	96.4	.932	.575	49.4	.269	.835
219.7	.965	.924	177.7	.992	.828	95.4	.948	.582	48.4	.279	.878
217.7	45.941	.937	175.7	.812	.787	94.4	44.973	.554	47.4	.307	.873
215.7	46.010	.948	173.7	.731	.742	93.4	45.089	.594	46.4	.253	.889
213.7	46.007	.957	171.7	.682	.716	92.4	.028	.578	45.4	.257	.894
211.7	45.999	.981	169.7	.629	.669	91.4	.024	.578	44.4	.318	.913
209.7	45.978	.986	167.7	.713	.659	90.4	.054	.620	43.4	.337	.931
207.7	46.006	.992	165.7	729	.620	89.4	.054	.629	42.4	.335	.935

TABLE 1 (cont.)

P	R_C	$R_\odot$	P	R_C	$R_\odot$	P	R_C	$R_\odot$	P	R_C	$R_\odot$
163.7	.637	.597	77.7	.876	.569	4.1	.462	.265	98.1	.770	.395
161.7	.624	.543	75.7	.852	.576	6.1	.462	.245	100.1	.780	.350
159.7	.849	.536	73.7	.893	.556	8.1	.418	.248	102.1	.817	.338
157.7	.819	.529	71.7	.847	.560	10.1	.512	.265	104.1	.688	.339
155.7	.710	.515	69.7	.812	.548	12.1	.527	.219	106.1	.652	.335
153.7	.767	.445	67.7	.776	.532	14.1	.571	.307	108.1	.640	.361
151.7	.730	.419	65.7	.808	.519	16.1	.581	.333	110.1	.623	.336
149.7	.667	.444	63.7	.775	.519	18.1	.602	.352	112.1	.602	.332
147.7	.616	.394	61.7	.799	.488	20.1	.589	.355	114.1	.596	.350
145.7	.546	.386	59.7	.728	.468	22.1	.564	.343	116.1	.676	333
143.7	.546	.359	57.7	.707	.467	24.1	.550	.348	118.1	.634	.317
141.7	.476	.336	55.7	.740	.459	26.1	.539	.323	120.1	.657	.306
139.7	.455	.310	53.7	.681	.458	28.1	.540	.346	122.1	.628	.298
137.7	.432	.307	51.7	.728	.477	30.1	.598	.296	124.1	.549	.269
135.7	.506	.286	49.7	.774	.449	32.1	.569	.314	126.1	.628	.264
133.7	.455	.280	47.7	.783	.444	34.1	.556	.342	128.1	.583	.220
131.7	.480	.286	45.7	.752	.413	36.1	.589	.348	130.1	.546	.222
129.7	.520	.247	43.7	.747	.448	38.1	.642	.340	132.1	.508	.211
127.7	.496	.225	41.7	.749	.455	40.1	.651	.382	134.1	.484	.217
125.7	.503	.192	39.7	.698	.440	42.1	.651	.367	136.1	.491	.163
123.7	.408	.148	37.7	.742	.440	44.1	.700	.400	138.1	.400	.171
121.7	.461	.116	35.7	.716	418	46.1	.743	.426	140.1	.374	.171
119.7	.427	.091	33.7	.720	.449	48.1	.772	.426	142.1	.379	.176
117.7	.353	46.055	31.7	.751	.424	50.1	.775	.420	144.1	.404	.186
115.7	.314	45.995	29.7	.779	.439	52.1	.768	.411	146.1	.363	.210
113.7	.176	.950	27.7	.760	.441	54.1	.707	.425	148.1	.420	.217
111.7	.142	.934	25.7	.762	.442	56.1	.756	.460	150.1	.458	.201
109.7	.101	.887	23.7	.734	.422	58.1	.770	.410	152.1	.448	.195
107.7	.046	.884	21.7	.759	.404	60.1	.749	.417	154.1	.383	.206
105.7	.082	.805	19.7	.727	.433	62.1	.759	.422	156.1	.326	.192
103.7	.066	.775	17.7	.712	.435	64.1	.837	.401	158.1	.374	.198
101.7	.137	.740	15.7	.743	446	66.1	.798	.384	160.1	.367	.177
99.7	.073	.727	13.7	.751	.462	68.1	.749	.387	162.1	.167	.141
97.7	45.036	.708	11.7	.741	.466	70.1	.761	.381	164.1	.207	.104
95.7	44.980	.689	9.7	.716	.471	72.1	.771	.383	166.1	.238	.067
93.7	45.033	.678	7.7	.744	.469	74.1	.809	.383	168.1	.204	.070
91.7	44.951	.631	5.7	.775	.482	76.1	.793	.361	170.1	.087	.093
89.7	.940	.631	3.7	.784	.495	78.1	.752	.398	172.1	.104	.076
87.7	.936	.643	1.7	.815	.555	80.1	.796	.373	174.1	.096	.055
85.7	.934	.626	359.7	.823	.577	82.1	.798	.399	176.1	.102	.047
83.7	.929	.622	357.7	44.987	.553	84.1	.828	.411	178.1	.019	.036
81.7	.914	.603	355.7	45.047	45.601	86.1	.775	.405	180.1	.052	.022
79.7	.914	.591				88.1	.856	.390	182.1	.016	.012
						90.1	.871	.406	184.1	45.097	46.021
		Film No. 71				92.1	.849	.408	186.1	44.972	45.992
356.1	45.872	46.306	0.1	.550	.259	94.1	.752	.412	188.1	.985	.974
358.1	.692	.275	2.1	.424	.257	96.1	.769	.408	190.1	44.982	.956

TABLE 1 (cont.)

P	$R_{\mathbb{C}}$	$R_{\odot}$	P	$R_{\mathbb{C}}$	$R_{\odot}$
192.1	45.008	.940	222.1	.819	.855
194.1	44.863	.909	224.1	.820	.856
196.1	.894	.917	226.1	.776	.850
198.1	.898	.908	228.1	.775	.806
200.1	.915	.947	230.1	.742	.808
202.1	.871	.941	232.1	.724	.786
204.1	.837	.936	234.1	.751	.781
206.1	.852	.884	236.1	.740	.789
208.1	.847	.890	238.1	.755	.786
210.1	.812	.881	240.1	.859	.774
212.1	.801	.899	242.1	.906	.774
214.1	.793	.888	244.1	.909	.776
216.1	.787	.882	246.1	44.943	.784
218.1	.806	.858	248.1	45.079	45.733
220.1	.744	.860			
		Film No. 72			
355.3	45.913	46.313	53.3	.526	.143
357.3	.729	.274	55.3	.544	.160
359.3	.613	.293	57.3	.568	.170
1.3	.556	.256	59.3	.552	.162
3.3	.520	.261	61.3	.588	.122
5.3	.581	.276	63.3	.622	.146
7.3	.568	.244	65.3	.578	.155
9.3	.536	.245	67.3	.616	.138
11.3	.526	.259	69.3	.601	.110
13.3	.554	.286	71.3	.617	.132
15.3	.595	.284	73.3	.653	.095
17.3	.600	.285	75.3	.627	.161
19.3	.646	.297	77.3	.597	.114
21.3	.631	.281	79.3	.628	.067
23.3	.632	.276	81.3	.662	.045
25.3	.596	.304	83.3	.618	.097
27.3	.581	.282	85.3	.597	.072
29.3	.664	.234	87.3	.580	.064
31.3	.546	.252	89.3	.616	.038
33.3	.600	.226	91.3	.553	46.033
35.3	.649	.230	93.3	.516	45.971
37.3	.620	.184	95.3	.453	.952
39.3	.614	.174	97.3	.404	.945
41.3	.572	.179	99.3	.442	.948
43.3	.660	.151	101.3	.413	.927
45.3	.649	.155	103.3	.320	.914
47.3	.635	.167	105.3	.258	.948
49.3	.653	.147	107.3	.202	.926
51.3	.585	.195	109.3	.209	.931
111.3	.202	.975	181.3	.024	46.004
113.3	.236	.935	183.3	.103	.006
115.3	.333	.941	185.3	.056	.041
117.3	.325	.946	187.3	.146	.090
119.3	.421	.939	189.3	.127	.070
121.3	.356	.958	191.3	.164	.114
123.3	.346	.938	193.3	.102	.121
125.3	.404	.912	195.3	.075	.130
127.3	.385	.922	197.3	.095	.148
129.3	.359	.947	199.3	.065	.106
131.3	.333	.926	201.3	.066	.135
133.3	.350	.964	203.3	45.002	.153
135.3	.303	.979	205.3	44.999	.137
137.3	.207	.983	207.3	.981	.136
139.3	.170	.981	209.3	.960	.166
141.3	.164	.961	211.3	.968	.131
143.3	.176	.931	213.3	.971	.109
145.3	.181	.930	215.3	.968	.092
147.3	.199	.933	217.3	.972	.092
149.3	.276	.955	219.3	.916	.099
151.3	.293	.955	221.3	.984	.119
153.3	.299	.964	223.3	44.999	.115
155.3	.230	.966	225.3	45.001	.162
157.3	.281	.934	227.3	44.966	.169
159.3	.288	.992	229.3	.974	.145
161.3	.119	.992	231.3	44.986	.161
163.3	.102	.974	233.3	.995	.161
165.3	.086	.955	235.3	45.012	.140
167.3	45.101	.960	237.3	.025	.156
169.3	44.991	45.981	239.3	.116	.134
171.3	44.997	46.001	241.3	.170	.174
173.3	45.046	46.000	243.3	.150	.154
175.3	45.092	45.978	245.3	.155	.116
177.3	44.995	.954	247.3	45.265	46.071
179.3	45.037	45.989			

NOTE: The position angles P shown in Table 1 for the 36th plate must be reduced by 6°.

/63 /62

TABLE 2

/64

P	$R_{\mathbb{C}}$	P	$R_{\mathbb{C}}$	P	$R_{\mathbb{C}}$
	Plate No. 52 (Crescent)				
346.2	54.110	300.2	.867	254.2	.842
345.2	.049	299.2	.850	253.2	.878
344.2	54.033	298.2	.884	252.2	.900
343.2	53.958	297.2	53.924	251.2	.811
342.2	54.016	296.2	54.006	250.2	.798
341.2	53.998	295.2	53.912	249.2	.868
340.2	53.989	294.2	.908	248.2	817
339.2	54.020	293.2	.851	247.2	.818
338.2	53.985	292.2	.865	246.2	.795
337.2	.985	291.2	.826	245 2	.793
336.2	53.959	290.2	.835	244.2	.805
335.2	54.001	289.2	.798	243 2	.794
334.2	53.921	288.2	.819	242.2	.868
333 2	.948	287.2	.770	241 2	.900
332.2	.893	286 2	.822	240 2	.910
331.2	.904	285.2	.825	239.2	.894
330.2	.838	284.2	.832	238 2	.853
329.2	.881	283.2	.800	237.2	.827
328.2	.789	282.2	.802	236.2	.791
327.2	.795	281.2	.812	235.2	.812
326.2	.842	280.2	.797	234.2	.840
325.2	.799	279.2	.855	233.2	.864
324.2	.807	278.2	.856	232.2	.811
323.2	.855	277.2	.891	231.2	.865
322.2	.870	276.2	.862	230.2	.842
321.2	.835	275.2	.835	229.2	.825
320.2	.879	274.2	.845	228 2	.853
319.2	.852	273.2	.841	227.2	.843
318.2	.878	272.2	.797	226 2	.850
317.2	.954	271.2	.786	225.2	.833
316.2	53 988	270.2	.786	224.2	.820
315.2	54.007	269.2	.714	223.2	.879
314.2	53.967	268.2	.754	222.2	.859
313.2	.951	267.2	.803	221.2	.892
312.2	.950	266.2	.795	220.2	.856
311.2	.963	265.2	.798	219.2	.821
310.2	.991	264.2	.861	218.2	.880
309.2	.959	263.2	.854	217.2	.887
308.2	.982	262.2	.841	216.2	.882
307.2	.932	261.2	.852	215.2	.868
306.2	.953	260.2	.836	214.2	.860
305.2	.924	259.2	.881	213.2	.848
304.2	.938	258.2	.811	212.2	.890
303.2	.946	257.2	.855	211.2	.887
302.2	.910	256.2	.818	210.2	.849
301.2	.885	255.2	.834	209.2	.874

TABLE 2 (cont.)

P	$R_{\mathbb{C}}$	P	$R_{\mathbb{C}}$	P	$R_{\mathbb{C}}$
208.2	.897	200.2	.944	193.2	.981
207.2	.903	199.2	.962	192.2	53.963
206.2	.878	198.2	.984	191.2	54.044
205.2	.894	197.2	.988	190.2	.041
204.2	.906	196.2	.937	189.2	.041
203.2	.932	195.2	.954	188.2	.064
202.2	.947	194.2	.882	187.2	54.126
201.2	.912				
	Plate No. 54 (Crescent)				
344.4	54.173	307.4	.064	270.4	.737
343.4	.129	306.4	54.046	269.4	.756
342.4	.172	305.4	53.994	268.4	.794
341.4	179	304.4	.988	267.4	.799
340.4	.205	303.4	.930	266.4	.786
339.4	.123	302.4	.913	265.4	.795
338.4	.166	301.4	.917	264.4	.798
337.4	.174	300.4	.926	263.4	.829
336.4	.110	299.4	.929	262.4	.877
335.4	.121	298.4	.914	261.4	.875
334.4	.053	297.4	.927	260.4	.906
333.4	.113	296.4	.907	259.4	.919
332.4	.045	295.4	.902	258.4	.918
331.4	54.014	294.4	.910	257.4	.888
330.4	53.972	293.4	.880	256.4	.877
329.4	.962	292.4	.888	255.4	.863
328.4	.957	291.4	927	254.4	.868
327.4	.933	290.4	.899	253.4	.846
326.4	.914	289.4	.889	252.4	.889
325.4	.954	288.4	.880	251.4	.855
324.4	53.977	287.4	.874	250.4	.873
323.4	54.014	286.4	.869	249.4	.856
322.4	54.030	285.4	.862	248.4	.853
321.4	53.960	284.4	.845	247.4	.852
320.4	.948	283.4	.852	246.4	.873
319.4	53.969	282.4	.859	245.4	.838
318.4	54.031	281.4	.898	244.4	.861
317.4	.047	280.4	.901	243.4	.842
316.4	.034	279.4	.883	242.4	.869
315.4	.022	278.4	.872	241.4	.888
314.4	.003	277.4	.852	240.4	.871
313.4	.011	276.4	.848	239.4	.881
312.4	.041	275.4	.850	238.4	.834
311.4	.065	274.4	.899	237.4	.851
310.4	.021	273.4	.889	236.4	.842
309.4	.041	272.4	.822	235.4	.824
308.4	.025	271.4	.776	234.4	.901

P	$R_{\mathbb{C}}$	P	$R_{\mathbb{C}}$	P	$R_{\mathbb{C}}$
233.4	.888	218.4	.792	203.4	.830
232.4	.860	217.4	.833	202.4	.859
231.4	.842	216.4	.867	201.4	.905
230.4	.848	215.4	.847	200.4	.888
229.4	.854	214.4	.804	199.4	.917
228.4	.851	213.4	.800	198.4	.898
227.4	.838	212.4	.800	197.4	.955
226.4	.807	211.4	.796	196.4	.957
225.4	.800	210.4	.767	195.4	.942
224.4	.823	209.4	.800	194.4	.874
223.4	.811	208.4	.810	193.4	.936
222.4	.780	207.4	.808	192.4	53.966
221.4	.833	206.4	.851	191.4	54.016
220.4	.830	205.4	.796	190.4	.009
219.4	.792	204.4	.827	189.4	54.009

DETERMINING CORRECTIONS FOR THE COORDINATES OF THE MOON ACCORDING TO OBSERVATIONS OF THE ANNULAR SOLAR ECLIPSE ON MAY 20, 1966

I.M. Demenko, A.S. Duma, D.P. Duma and V.S. Kislyuk

In preparing for observations of solar eclipses, special attention was paid to setting the tube of the coronagraph in a given direction. To compute the azimuth, we know of several formula systems [1-4] suitable for instruments with movable lenses. However, our expedition was equipped with coronagraphs with immovable lenses. In these instruments the reflected solar beam is directed in an invariable horizontal direction by rotating a plane mirror in front of the lens around an axis parallel to the Earth's axis. We propose that simple formulas be used to compute the azimuth of a coronagraph with an immovable lens. /67

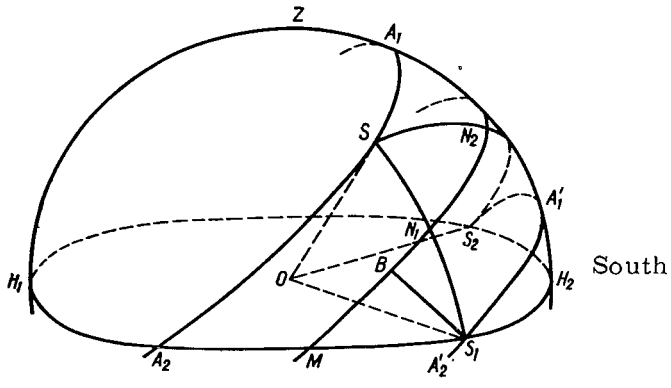

Fig. 1.

In an ideal arrangement for the coelostat mirror, the normal to the mirror ON always lies in the plane of the celestial equator MN_1N_2 (Fig. 1). Therefore, a beam from point S with declination $+\delta$ intersects the celestial sphere at a point with declination $-\delta$ after reflecting off the mirror. If A_1A_2 is the diurnal parallel of point S, then the circular arc $A_1'A_2'$ will be its reflection. With $\delta_S \leq 90^\circ - \phi$ (ϕ is the latitude of the observation site) the circular arc $A_1'A_2'$ intersects the line of the horizontal at two points S_1 and S_2 corresponding to the two positions of the mirror. If the Sun is at point S, then to observe the Sun the optical axis of the coronagraph must be set in one of two directions: OS_1 or OS_2. The azimuth A of the coronagraph can be computed from the right spherical triangle MS_1B, in which $\angle BMS_1 = 90^\circ - \phi$, $MS_1 = k = 90^\circ - A$, $BS_1 = |\delta|$. The desired formula has the form /68

$$\cos A = \sec \varphi \sin (\delta_\odot + \Delta\delta_\odot), \tag{1}$$

where $\delta_\odot$ is the geocentric declination of the Sun at the moment of observation; $\Delta\delta_\odot$ is declination correction for refraction.

The correction $\Delta\delta_\odot$ is computed according to the known formula

$$\Delta\delta_\odot = \frac{k(\sin\varphi\cos\delta_\odot - \cos\varphi\sin\delta_\odot\cos t_\odot)}{\sin\varphi\sin\delta_\odot + \cos\varphi\cos\delta_\odot\cos t_\odot}, \tag{2}$$

which for ease of computation is best transformed to

$$\Delta\delta_\odot = \frac{k(\cot\delta_\odot - \cot\varphi\cos t_\odot)}{1 + \cot\varphi\cot\delta_\odot\cos t_\odot}. \tag{3}$$

Here k is the coefficient of refraction, $t_\odot$ is the hourly angle of the Sun. Formula (1) has two solutions, but the tube of the coronagraph is directed toward that section of the sky (east or west) in which the Sun is located.

Since the Sun does not move in a direction parallel to A_1A_2, its image in the plate will shift along an arc other than $A_1'A_2'$ at a rate of

$$v = 2v_\odot \sin\frac{\gamma}{2}, \tag{4}$$

where $v_\odot = 15F\cos\delta_\odot \sin 1'$ mm/min (the speed of the image with a fixed mirror); F is the focal length of the lens in mm; γ is the angle on the plate between the direction of the diurnal parallel of point S and the visible direction in which the Sun is moving. This angle takes into account the influence of refraction and the annual motion of the Sun [2].

Before the observation we must also know the value of the shift in the Sun's image on the plate during the eclipse. If the shift from the beginning to the end of the eclipse is large (the Sun leaves the plate), then the azimuth of the coronagraphs must be computed for the midpoint of the eclipse. In our case, the azimuth of the coronagraphs at the midpoint of the eclipse was equal to 60°20'.

There are several methods for analyzing the data to determine corrections for the coordinates of the Moon according to observations of a solar eclipse. /69

In one of these methods, the coordinate correction is computed on the basis of the difference between the observed and computed moments of the disc contacts. The results of this method are not very accurate, since the moments of contact cannot be recorded with certainty. More precise results can be obtained by using other methods which measure the width of the solar crescent near the center line or the length of the chord which subtends the endpoints of the solar crescent.

We determined corrections for the coordinates of the Moon based on measurements of the ring width. The choice of the ring was deemed advisable for the following reasons.

(1) The ring contains more diametrically opposed points than the crescent. Therefore, if we measure the ring, both coordinates can be determined with identical accuracy.

(2) The position angle of the line connecting the centers of the Sun and the Moon varies within a wide range near the greatest phase. Therefore, the coefficients in the conventional equations have different signs and a value which renders a certain separation of the unknown variables necessary.

To determine corrections for the coordinates of the Moon, we chose 14 rings (7 plates and 7 films) obtained on the 12- and 10-meter coronagraphs. Basic information concerning the quality of the observational data is contained in [10].

The negatives were measured on a UIM-22 microscope in polar coordinates. Using a stencil with concentric circles and a sharp needle, we placed a mark on the negative as close as possible to the center of the Sun. The films were fixed on the stage of the microscope between clean transparent slides. The negatives were centered in such a way that at all angles of rotation of the negative, the mark remained in the center of the cross-hairs. The measurements were taken only along one longitudinal scale rotating the position circle by 1 or 2° at a time, beginning from the end point of the ring. We took two readings on the mark and four on the limbs of the Sun and the Moon. The photographs were measured at only one position on the microscope stage.

To compute corrections for the coordinates of the Moon we must know the measured distance between the centers of the Sun and the Moon. This distance was found by measuring the widths of the solar ring in the following way.

In rectangular coordinate system xoy (o is the center of the Sun, the x axis is directed toward the north pole and the y axis toward the east on the Moon), the coordinates of the center of the Moon Δx, Δy and the ring width Δh_i are related by the expression /70

$$\Delta x \cos P + \Delta y \sin P + \Delta h_0 = \Delta h - \Delta h_i. \qquad (5)$$

The position angles P of the limb points, computed from the north pole of the Moon, were found from measured angles after the negative of the lunar limb was identified with the Weimer profiles [5]. We introduced a correction to the measured ring width on the plates for distortion of the solar limb [10].

The average thickness of the ring is determined by the formula

$$\Delta h = \frac{1}{n}\sum_{i=1}^{n}\Delta h_i, \qquad (6)$$

where n is the number of measurements.

The distance σ_0 between the centers of the Sun and the Moon and the position angle of the Moon relative to the Sun, computed from the circle of declinations to the east, can be calculated according to the formulas

$$\sigma_0 = \sqrt{\Delta x^2 + \Delta y^2},$$
$$P = \arctan\frac{\Delta y}{\Delta x} + C, \qquad (7)$$

where C is the topocentric position angle of the axis of rotation of the Moon at the moment of observations.

To determine corrections for the lunar coordinates, it is necessary to compare the observed and ephemeris positions of the Sun and the Moon. To do this we determined the ephemeris positions of the Sun and the Moon at the moment of observation. Their geocentric coordinates were interpolated directly from the 1966 Astronomical Yearbook of the USSR. To convert from universal time to ephemeris time, we took the preliminary correction ΔT = +35.86 sec. No other corrections were introduced into the ephemeris values of the lunar and solar coordinates. Conversion to topocentric positions was accomplished according to known formulas which take parallax into account.

Let us introduce for reference some values which we used in our calculations:

annular phase	T = 11 hrs. 06 min 46.48 sec;
topocentric libration	l' = 5.89°;
	b' = 0.06°;
topocentric position angle of the lunar axis of rotation	c' = 11.06°; /71
topocentric radii	$R'_\odot$ = 949.78";
	$R'_\mathbb{C}$ = 941.97";
zenith distances	$z_\odot$ = 59°45'13.80";
	$z_\mathbb{C}$ = 59°45'15.71";
parallax angle	$q_\odot$ = 47°51'49.44";
	$q_\mathbb{C}$ = 47°51'50.00";
partial phase (54th film)	T = 11 hrs 23 min 26.77 sec;
topocentric radius	$R'_\mathbb{C}$ = 941.42";
zenith distance	$z_\mathbb{C}$ = 62°33'04.63";
parallax angle	$q_\mathbb{C}$ = 47°54'04.63";

pressure B = 727.5 mm%;
temperature t = +23.0°C.

TABLE 1. POLAR COORDINATES OF THE MOON

No.	Photograph No.	T	$P_{\mathbb{C}}$	σ_0	σ_c	$\Delta\sigma$
			Plates			
1	32	11 h 06 m 36.95 s	271° 53.6	5.747″	7.487″	−1.740″
2	34	42.84	280 54.0	4.162	5.115	−0.953
3	35	46.48	290 53.5	2.009	3.713	−1.704
				2.016		−1.697
				2.256		−1.457
4	36	49.31	304 59.0	1.450	2.764	−1.314
5	38	56.24	17 28.5	2.873	2.331	+0.542
6	39	59.14	36 35.4	3.611	3.383	+0.228
7	40	07 01.64	46 11.8	4.231	4.187	+0.044
			Films			
8	66	11 06 39.415	275 05.8	6.682	6.497	+0.192
9	67	43.163	281 13.0	5.610	4.992	+0.618
10	68	47.276	294 23.2	3.589	3.403	+0.186
11	69	53.180	343 30.9	1.759	2.104	−0.345
12	70	56.948	23 41.0	2.691	2.558	+0.133
13	71	07 00.680	43 43.6	4.521	3.940	+0.581
14	72	04.394	54 15.2	6.388	5.260	+1.128

The results of the ephemeris calculations are given in Table 1, which uses the following notations: $T = UT + T$ (the time of the midpoint of the exposure); $P_{\mathbb{C}}$ is the position angle of the Moon relative to the Sun; σ_0, σ_s are the distances between the centers of the Sun and the Moon according to observations and ephemeris: $\Delta\sigma = \sigma_0 - \sigma_s$. /72

Figure 2 shows the path of the center of the Moon across the disc of the Sun. Here (1) shows the ephemeris path; (2) shows the visible path (from the 12-meter coronagraph, [●]); (3) shows the visible path (from the 10-meter coronagraph [○]). It can be seen that there is a satisfactory agreement between the results.

Corrections for the lunar coordinates were computed according to the rather rigorous formulas

$$\frac{\cos\delta_{\mathbb{C}}}{f\sin P_{\mathbb{C}}}\Delta\alpha_{\mathbb{C}} - \sigma_0\zeta = \sigma_0 - \sigma_c; \tag{8}$$

$$\frac{1}{f\cos P_{\mathbb{C}}}\Delta\delta_{\mathbb{C}} - \sigma_0\zeta = \sigma_0 - \sigma_c, \tag{9}$$

where $\Delta\alpha_{\mathbb{C}}$, $\Delta\delta_{\mathbb{C}}$ are the unknown corrections of the direct ascensions and declinations of the Moon; ζ is the correction for the scale of the negatives (per 1 mm 17.362″ for plates and 20.640″ for films);

f = 0.99153 is the coefficient of conversion from topocentric to geocentric coordinates.

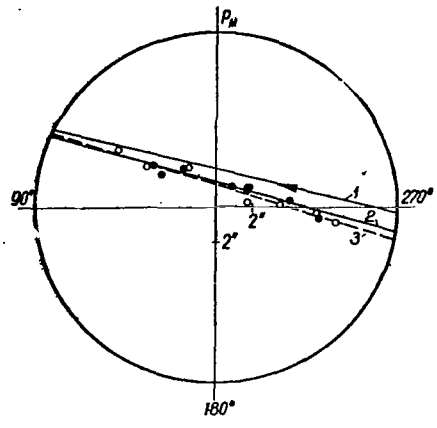

Fig. 2.

Table 2 shows the solution to conventional equations (8) and (9) according to the data in Table 1.

For the total series of observations (plates and films), both systems of equations (8) and (9) were reduced to a single system and all the conventional equations were assigned equal weight.

Analysis of the corrections leads to the following conclusions.

(1) The accuracy in our determination of the corrections for the lunar coordinates is almost an order of magnitude higher than the determination in [6-9]. This is explained by the fact that we investigated rings which cover longer arcs of the lunar limb than the crescents used in [6-9] for this purpose. In the investigation of the crescents, the center of the Moon was determined according to half the visible disc of the Moon. As a result, the coordinates of the center of the figure do not coincide for different photographs. When all the crescents are reduced to a single series to solve the equations, the determination of the /73 corrections for the coordinates becomes less reliable than the determination using rings because of a certain east-west asymmetry of the lunar disc which was not taken into account.

TABLE 2. CORRECTIONS FOR THE LUNAR COORDINATES

Coordinates	Plates	Films	Plates and Films
$\Delta\alpha_{\mathbb{C}}$	$+0.039\pm0.008^{s}$	$+0.008\pm0.003^{s}$	$+0.021\pm0.009^{s}$
$\Delta\delta_{\mathbb{C}}$	$-0.04''\pm0.03''$	$-0.10''\pm0.01''$	$-0.06''\pm0.03''$
$\Delta\lambda_{\mathbb{C}}$	$+0.52\pm0.11$	$+0.09\pm0.01$	$+0.28\pm0.13$
$\Delta\beta_{\mathbb{C}}$	-0.16 ± 0.01	-0.12 ± 0.01	-0.12 ± 0.01
ζ_8	$+0.24\pm0.05$	-0.10 ± 0.02	-0.01 ± 0.04
ζ_9	$+0.12\pm0.15$	-0.18 ± 0.01	
σ_8	$\pm0.52''$	$\pm0.22''$	±0.91
σ_9	±1.10	±0.08	

(2) It follows from Table 2 that the corrections for the lunar coordinates using the plates were not determined as accurately as those using the films, and these corrections do not agree among themselves. This may be explained by the following facts.

The rings from the 12- and 10-meter coronagraphs were incomplete and cover sections of the ring extending 311°-0°-210° and 356°-0°-247°, respectively. In view of the asymmetry of the Moon, the centers of the probable circles discovered by the observers will not coincide. The latter is reflected in the convergence of the coordinate corrections.

The moments of time were recorded on the 12- and 10-meter coronagraphs by printing and recording chronographs, respectively. During the annular phase, when all the equipment was operating under maximum load, the voltage in the power system fell somewhat. We noticed from the sound that the motor of the printing chronograph was not always operating at the necessary regime. It is possible that the rotation rate of the chronograph drum was not constant. The change in the behavior of the chronograph was taken into account by linear interpolation. Therefore, the exposure times contain some errors.

There were contacts on the tape of the recording chronograph every second. Therefore, errors in the exposure times for the above-mentioned reasons are practically absent. We should therefore assume that the results from the data of the 10-meter chronograph are more reliable. /74

(3) The 1966 Astronomical Yearbook of the USSR contained as a preliminary value for 1966 a value for the correction to the ephemeris time of ΔT = 35.0 sec.

Based on observations of the solar eclipse for May 20, 1966 are the following corrections:

12-meter coronagraph $\Delta T = 36^{s}.89 \pm 0^{s}.24$

10-meter coronagraph $\Delta T = 36^{s}.07 \pm 0^{s}.09$

overall result $\Delta T = +36^{s}.42 \pm 0^{s}.27$

All values of ΔT contain corrections for the ephemeris of the Sun and the Moon.

References

1. Vsekhsvyatskiy, S.K., Ye.Ya. Bugoslavskaya and A.N. Deych: In the Book: Trudy ekspeditsiy po nablyudeniy polnogo solnechnogo zatmeniya 19 iyunya 1936 goda (Proceedings of Expeditions to Observe the Total Solar Eclipse of June 19, 1936). Academy of Sciences of the USSR Press, Moscow-Leningrad, Ch. 1, 1938.
2. Lengauer, G.G.: In the Book: Trudy ekspeditsiy po nablyudeniy polnogo solnechnogo zatmeniya 19 iyunya 1936 goda (Proceedings of Expeditions to Observe the Total Solar Eclipse of June 19, 1936). Moscow-Leningrad, Academy of Sciences of the USSR Press, Ch. 2, 1939, p. 123.
3. Bugoslavskaya, Ye.Ya.: In the Book: Trudy GAISh (Proceedings of the Shternberg State Astronomical Observatory). Ch. 19, 1950.
4. Marinbakh, A.B.: Bull. of the All-Union Astronomical and Geodetic Society, Academy of Sciences of the USSR Press, Moscow, Vol. 32, No. 39, 1962.
5. Weimer, T.: Atlas de profiles lunaires (Atlas of Lunar Profiles). Paris, 1952.
6. Lengauer, G.G.: In the Book: Trudy ekspeditsiy po nablyudeniy polnogo solnechnogo zatmeniya 19 iyunya 1936 goda (Proceedings of Expeditions to Observe the Total Solar Eclipse of June 19, 1936). Academy of Sciences of the USSR Press, Moscow-Leningrad, Ch. 2, 1939, p. 129.
7. Gusev, N.G.: In the Book: Trudy ekspeditsiy po nablyudeniy polnogo solnechnogo zatmeniya 21 sentyabrya 1941 goda (Proceedings of Expeditions to Observe the Total Solar Eclipse of September 21, 1941). Academy of Science of the USSR Press, Moscow-Leningrad, 1949.
8. Vsekhsvyatskiy, S.K. and I.I. Il'inskiy: In the Book: Trudy ekspeditsiy po nablyudeniy polnogo solnechnogo zatmeniya 21 sentyabrya 1941 goda (Proceedings of Expeditions to Observe the Total Solar Eclipse of September 21, 1941). Academy of Sciences of the USSR Press, Moscow-Leningrad, 1949, p. 262.
9. Gavrilov, I.V. and I.G. Kolchinskiy: Polnyye solnechnyye zatmeniya 25 fevralya 1952 i 30 iyunya 1954 goda (The Total Solar Eclipses of February 25, 1952 and June 30, 1954). In the Book: Trudy ekspeditsiy (Proceedings of the Expeditions). Academy of Sciences of the USSR Press, Moscow, 1958.
10. Demenko, I.M., A.S. Duma and D.P. Duma: The Lunar Profile According to Observations of the Annular Solar Eclipse of May 20, 1966 (cf. this issue).

THE ACCURACY OF THE DETERMINATION OF THE COORDINATES OF THE SITE AND THE MOMENTS OF OBSERVATION OF THE ANNULAR SOLAR ECLIPSE OF MAY 20, 1966

N.A. Vasilenko

The path of the annular solar eclipse of May 20, 1966 passed /76 over the territory of the Soviet Union through the southern regions of Kazakhstan, the northern Caucasus, the Black Sea and, according to preliminary calculations, did not exceed 22 km in width. The small dimensions of the path of the visible annular phase (and the duration of the phase itself) placed certain restrictions on the choice of the observation site. After surveying the projected section of the path, we chose the village of Oytagan of the Aksus region in the Alma-Ata oblast. The observation area was chosen with the help of a detailed topographical chart. The equipment and instruments of the expedition were set up on the left bank of the Aksu River 300 m to the east of the village. The operating area of the expedition was a flat, semiarid region with very sparse ground cover. For 3-4 km to the north and west we could see the sands of the southern Pribalkhash'ya (Ishikotrau).

To determine the site coordinates and the moments of observation of the solar eclipse, the expedition was equipped with a UV 2"/2" EOMZ TsNIIGAiK universal instrument, two class-2, brand 6MKh naval chronometers (a No. 8626 stellar and a No. 1141 mean chronometer), two chronographs (one which recorded numbers and a tracing chronograph), an all-wave type PRV receiver, a pulse device to automatically receive radio signals within a precise time, an aneroid barometer and thermometers.

The equipment was set up in a field and from May 1, we began to receive second signals to check the behavior of the chronometers. The receiver, the chronometers and the recording chronograph were set up on a specially equipped platform, protected from solar rays by a canopy made of sheets of veneer and protected from the wind by the wall of an old existing structure. To eliminate the effects of a drastic change in temperature caused by a change in the weather of transition from day to night, the chronometers were covered with felt. Bihourly variations in the behavior of the chronometers caused by temperature changes did not exceed 0.1 sec. The second signals were received on the tape of the chronograph using a pulse device. The tape of the chronograph could be read with an accuracy of 0.01

sec. The moments of the eclipse on the 12-meter coronograph were recorded using the recording chronograph. The tape of the chronograph received precise second signals at the beginning and end of the observations. The moments of observation on the 10-meter coronagraph were timed on a stellar chronometer using the tracing chronograph. The tape of this chronograph could be read with an accuracy of 0.01 sec using a special measurement device. The precise time signal was received from the Moscow-time radio signal (Moscow). Let us now present the moments at which the signals were received and the determinations of the chronometer corrections during the observation of the solar eclipse. /77

Local Time	Operation
14 hrs 24 min	Signal Reception
14 28	Determination of the Correction of Chronometer No. 1141
14 34	Determination of the Correction of Chronometer No. 8626
15 29	Determination of the Correction of Chronometer No. 1141
15 33	Determination of the Correction of Chronometer No. 8626
16 07	Signal Reception
17 54	Signal Reception
18 08	Determination of the Correction of Chronometer No. 8626
18 21	Signal Reception
18 25	Determination of the Correction of Chronometer No. 8626
18 33	Determination of the Correction of Chronometer No. 1141

The astropoint was determined on a brick column with dimensions of 50 × 50 × 120 cm above the surface of the Earth and 60 × 60 × 100 cm below the surface of the Earth.

To determine hourly corrections, we observed 23 Singer pairs. Over two evenings we determined three longitudes according to the A § 209 programs of instruction of the Main Administration of Geodesy and Cartography [1]. The moments of passage were recorded on the tape of the chronagraph by the "eye-key" method. The final value for longitude was found with a mean square error of $\sigma_2 = \pm 0.02$ sec. The latitude was determined over three evenings by observing 20 Talcott pairs with constant filaments. The final value for latitude was found from equalizing calculations. When the latitude was equalized, we determined the correction by the value of the scale of the revolution of an ocular micrometer at the moment of observation ($\Delta R = -0.132''$) and the correction for the mean value of latitude ($\Delta\phi = -0.233''$). The equalized value of the latitude was derived with a weight $P_\phi = 9.2$ with $P_{\phi_{prelim}} = 3.2$ (permissible for this instrument), which indicates the overall program of the Talcott pairs was properly compiled. /78

The mean square error in determining the latitude of the astropoint according to the internal consistency of the results of individual pairs was $\sigma'_\phi = \pm 0.95''$. The final (equalized) latitude value was obtained with a mean square error of $\sigma_\phi = \pm 0.31''$. The determinations of the longitude and latitude of the astropoint were interpreted according to the standard systems given in Tables 59 and 80 [2]. The coronagraphs were tied in by the polar method according to the measured distances and the azimuth between the astropoint and the lenses of the coronagraphs (for the 12-meter d = 47 m, A = 166° and for the 10-meter, d = 50 m and A = 167°).

Thus the coordinates of the location of the coronagraphs were determined with errors:

latitude $\sigma_\phi = \pm 0.31''$;
longitude $\sigma_\lambda = \pm 0.02$ sec.

In this determination we assumed that the tie-in between the coronagraphs and the astropoint was sufficiently high and would not increase the errors in σ_ϕ and σ_λ corresponding to the coordinates of the astropoint.

References

1. Instruktsii o postroyenii gosudarstvenooy geodezicheskoy seti Soyuza SSR (Instructions for Constructing the State Geodetic Network of the USSR). Gostekhizdat, Moscow, 1961.
2. Trudy TsNIIGAiK (Proceedings of the State Scientific Research Institute for Geodesy, Astronomy and Cartography). Moscow, Gostekhizdat, 1962, p. 148.

DESCRIPTION OF THE HIGH-SPEED CASSETTE AND SHUTTER USED TO OBSERVE THE ANNULAR SOLAR ECLIPSE OF MAY 20, 1966

K.Ye. Skorik

The astronomical expedition of the Main Astronomical Observatory, in its observations of the annular solar eclipse of May 20, 1966, faced the problem of obtaining the largest number of photographs covering the entire period of the eclipse from the 1-st to the 4-th contacts and also, and this was of utmost importance, at the moments of the annular phase. This need gave rise to increased demands on the high-speed capability of the astronomical instruments, in particular: /79

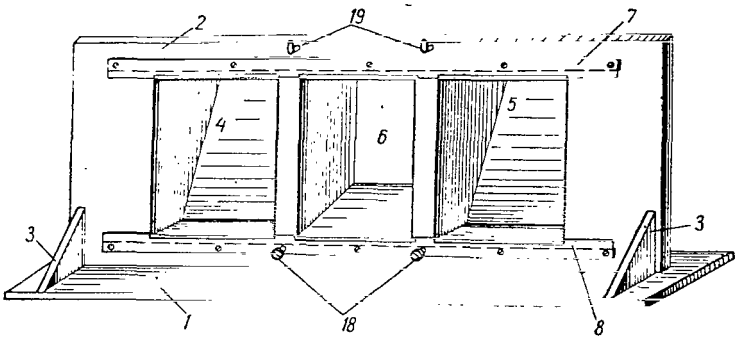

Fig. 1.

(a) equipping the observation instruments with high-speed cassettes for use with photographic plates 18 × 24 cm and a reloading speed of less than 1 sec;

(b) a high cassette capacity (25-30 plates) to obtain the necessary number of photographs;

(c) high-speed shutters for the prescribed photographic plate dimension and exposure times of from 1/50 to 1/1000 sec and less.

There were no industrial prototypes of the cassettes and shutters satisfactory for our purposes. Therefore, for this expedition, the experimental-mechanical department of the Main Astronomical

Observatory of the Academy of Sciences of the Ukrainian SSSR devel- /80
oped and produced the necessary cassettes and shutters; they are described below.

The Cassette Section. The base of the cassette section (1) and the vertical plate (2), to which we attached the moving parts of the cassette, were made of 20-millimeter veneer, fastened together with angle brackets (3) (Fig. 1). The vertical plate (2) had three openings, two of which (19 × 25 cm) were used as receiving pockets (4) and (5). The third was the shutter aperture (6) (17 × 23 cm). Above and below the openings we installed two guide runners (7) and (8) which held a frame (9) (Fig. 2) which had two pins (10) to hold it in place. The frame had to be 0.3-0.5 mm thinner than the photographic plates used. The height of the frame h corresponded to one dimension of the plate and the width l is 4 mm larger than the second dimension of the plate. The frame had handles (11) to move it through the guide runners. The photographic plate was loaded into the cassette (12) (Fig. 3). The cassette was made of duralumin and had mounting brackets (13) and a removable internal floor (14) (shown by the dotted line). Springs (15), which were set in sleeves (16), press the movable floor against the vertical plate (2) (cf. Fig. 1), which is located in the focal /81 plane of the lens. We nailed a cover made of black material around the perimeter of plate (2) with two handles for easy operation by the observer. If the cassette section was kept in the tent, no material light-shield was needed.

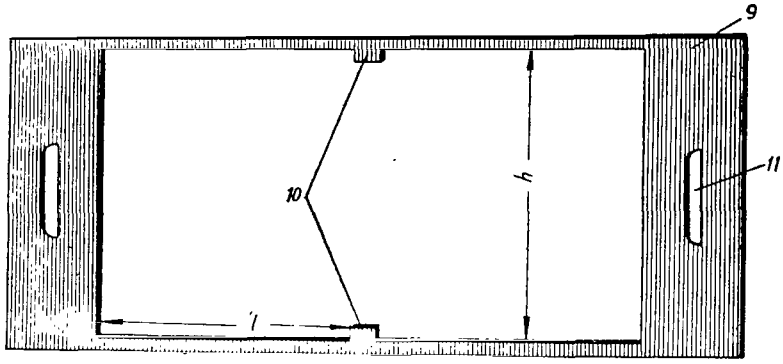

Fig. 2.

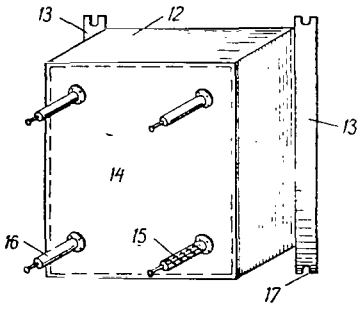

Fig. 3.

The cassette was loaded and operated in the following way. A total of 25-30 plates (for one loading) were lightly pasted together using black paper in a direction opposite to that of the solar corona. The plates were then inserted into the cassette (12) which compressed the springs (15). Then the lower lugs (17) were fitted to screws (18); the upper part of the cassette was held in place by wing nuts (19) (cf. Fig. 1). To do this, the frame (9) must be in the extreme left or extreme right position. After exposure the observer moves the frame from one

extreme position to the other. The lugs (10) hold the exposed plate which then falls into one of the receiving pockets (4) or (5), and the next plate is fed into the focal plane. When the frame (9) is moved in the opposite direction, the reloading operation is repeated. The efficiency of this type of cassette is rather high. Exposure of thirty plates with short exposure times requires less than one minute. The inconvenience in operating this type of cassette lies in the fact that preliminary preparation of the plates is necessary before the observations. /82

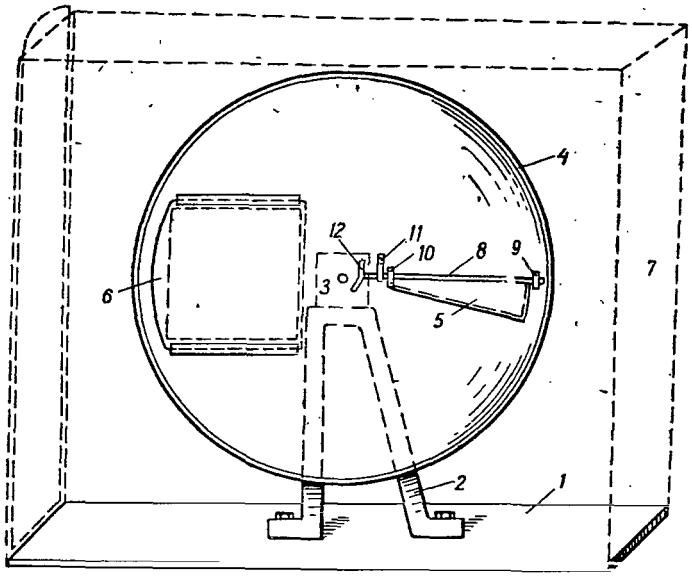

Fig. 4.

The Shutter. An angle bracket (2) made of angled steel (30 × 30 mm) is attached to a horizontal panel (1) (Fig. 4). A motor (3) is attached to the upper part of the bracket. The shaft of the motor turns a disc (4) 750 mm in diameter made of 0.5 duralumin; a steel wire was installed around the perimeter to induce the necessary voltage. The disc had two apertures: one in the form of a sector variable from 1 to 5° closed by a flag (5) of the same shape, and the second in the form of a rectangle 18 × 24 cm opened and closed by a screen (6) and necessary to focus and align the coronagraph. After installation the disc was dynamically balanced. The shutter was enclosed in a lightproof container (7) and connected to the cassette section and the tube of the coronagraph by cloth sleeves. The shutter was placed on a separate base directly adjacent to the cassette section to prevent the transfer of vibrations to the cassette section of the /83

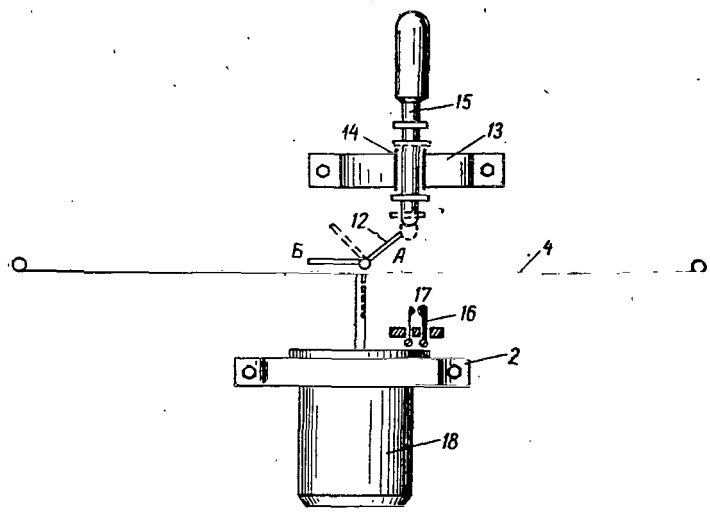

Fig. 5.

coronagraph. The flag (5) was attached to an axle (8) which rotated on two bronze bearings (9) and (10). The end of the flag axle, rotating toward the center of the disc, included a square in its cross section held by two plane springs (11). Thus the flag can be accurately fixed in two positions: (a) shutter closed, and (b) shutter open (i.e., the flag is perpendicular to the plane of the disc). At the very end of the axle (8) we attached a double arm (12) (Fig. 5, upper view), which was used to rotate the flag. On the other side of the disc we installed a frame (13) which held a bronze bushing (14) in which the shaft shifted freely.

The shutter operated in the following way: when the disc was rotating the flag (5) was closed. To expose a plate, we simply pushed button (15) briefly which then occupied the position shown in Figure 5 by the dotted line. The end of the double arm (A), hit by the end of the shaft, tilted and rotated the axle (8). At the same time, the arm pushed the shaft and returned it to its initial position. The double arm would take the position shown in Figure 5 by the dotted line, the sector would be opened and the exposure completed. As soon as the sector passed the plate, the other end of the double arm B would hit the pin (16), the rotating axle (8) and the flag would shut the aperture in the disc. At the same time contacts (17) would be closed, engaging the recording chronograph which would print the moment the exposure ended on the tape. The process would be repeated for the next exposure. The value of the sector did not vary during the observations, but the exposure time could be varied by regulating the rotation rate of the disc. A shunt-type electric motor (18) with a voltage of 24 V was fed from a VSA-5 rectifier across a C-0.7 ferroresonance stabilizer. The rotation rate of the disc was regulated by varying the voltage. With a particular choice for the value of the sector and rotation rate of the disc, we were able to obtain exposure times of 1/100 sec and less.

The shutter and cassette described above, used to observe the annular solar eclipse, were very convenient to use and reliable in their operation.

Translated for the National Aeronautics and Space Administration by:
Aztec School of Languages, Inc.
Research Translation Division (179)
Maynard, Massachusetts and McLean, Virginia
NASW-1692

NATIONAL AERONAUTICS AND SPACE ADMINISTRATION
WASHINGTON, D.C. 20546

OFFICIAL BUSINESS

FIRST CLASS MAIL

POSTAGE AND FEES PAID
NATIONAL AERONAUTICS AND
SPACE ADMINISTRATION

04U 001 55 51 3DS 70185 00903
AIR FORCE WEAPONS LABORATORY /WLOL/
KIRTLAND AFB, NEW MEXICO 87117

ATT E. LOU BOWMAN, CHIEF,TECH. LIBRARY

Undeliverable (Section 158
Postal Manual) Do Not Return

"The aeronautical and space activities of the United States shall be conducted so as to contribute . . . to the expansion of human knowledge of phenomena in the atmosphere and space. The Administration shall provide for the widest practicable and appropriate dissemination of information concerning its activities and the results thereof."

—NATIONAL AERONAUTICS AND SPACE ACT OF 1958

NASA SCIENTIFIC AND TECHNICAL PUBLICATIONS

TECHNICAL REPORTS: Scientific and technical information considered important, complete, and a lasting contribution to existing knowledge.

TECHNICAL NOTES: Information less broad in scope but nevertheless of importance as a contribution to existing knowledge.

TECHNICAL MEMORANDUMS: Information receiving limited distribution because of preliminary data, security classification, or other reasons.

CONTRACTOR REPORTS: Scientific and technical information generated under a NASA contract or grant and considered an important contribution to existing knowledge.

TECHNICAL TRANSLATIONS: Information published in a foreign language considered to merit NASA distribution in English.

SPECIAL PUBLICATIONS: Information derived from or of value to NASA activities. Publications include conference proceedings, monographs, data compilations, handbooks, sourcebooks, and special bibliographies.

TECHNOLOGY UTILIZATION PUBLICATIONS: Information on technology used by NASA that may be of particular interest in commercial and other non-aerospace applications. Publications include Tech Briefs, Technology Utilization Reports and Notes, and Technology Surveys.

Details on the availability of these publications may be obtained from:

SCIENTIFIC AND TECHNICAL INFORMATION DIVISION

NATIONAL AERONAUTICS AND SPACE ADMINISTRATION

Washington, D.C. 20546